INVESTIGATION OF LOCAL RAW MATERIALS FOR THE PRODUCTION OF LITHIUM-ION BATTERY SEPARATORS IN THAILAND

PANALEE KERDTHONG

MASTER OF SCIENCE
IN
MATERIALS INNOVATION FOR SUSTAINABILITY

SCHOOL OF SCIENCE
MAE FAH LUANG UNIVERSITY
2025

INVESTIGATION OF LOCAL RAW MATERIALS FOR THE PRODUCTION OF LITHIUM-ION BATTERY SEPARATORS IN THAILAND

PANALEE KERDTHONG

THIS THESIS IS A PARTIAL FULFILLMENT OF THE REQUIREMENTS FOR THE DEGREE OF MASTER OF SCIENCE IN MATERIALS INNOVATION FOR SUSTAINABILITY

SCHOOL OF SCIENCE
MAE FAH LUANG UNIVERSITY
2025

THESIS APPROVAL

MAE FAH LUANG UNIVERSITY

FOR

MASTER OF SCIENCE

IN

MATERIALS INNOVATION FOR SUSTAINABILITY

Thesis Title: Investigation of Local Raw Materials for the Production of Lithium-ion Battery Separators in Thailand

Author: Panalee Kerdthong

Examination Committee:

Associate Professor Sukum Eitssayeam, Ph. D.	Chairperson
Assistant Professor Sitthi Duangphet, Ph. D.	Member
Assistant Professor Uraiwan Intatha, Ph. D.	Member
Associate Professor Nattakan Soykeabkaew, Ph. D.	Member
Assistant Professor Nattaya Tawichai Ph. D.	Member

Advisors:

.....Advisor
(Assistant Professor Sitthi Duangphet, Ph. D.)

.....Co-Advisor
(Assistant Professor Uraiwan Intatha, Ph. D.)

.....Co-Advisor
(Associate Professor Nattakan Soykeabkaew, Ph. D.)

Dean:

.....
(Professor Surat Laphookhieo, Ph. D.)

ACKNOWLEDGEMENTS

Writing this dissertation would not have been possible without the generous support and encouragement of many individuals and organizations. First and foremost, I would like to express my sincere gratitude to Mae Fah Luang University and the National Research Council of Thailand (NRCT) for their financial support through Grant No. N23D650045. Their contribution made this research possible and provided the foundation for the successful completion of this work.

I would also like to extend my heartfelt appreciation to IRPC Public Company Limited, Thailand, for their generous support in providing access to machinery, equipment, and testing facilities, as well as their valuable technical assistance throughout the study. My special thanks go to the Synchrotron Light Research Institute (Public Organization), Thailand, for granting access to their facilities and for their essential support in the 2D-WAXS analysis. I would also like to thank the Office of Postgraduate Studies, Mae Fah Luang University, for supporting this research through the Research and Publishing Grants (grant no. 0404 and 0281).

Finally, I would like to express my sincere thanks to the Electro-Ceramics Research Laboratory, Faculty of Science, Chiang Mai University, Thailand, for their kind cooperation and continuous support during the research process. It is through the guidance, encouragement, and contributions of these institutions and individuals that I was able to bring this dissertation to completion successfully.

Panalee Kerdthong

Thesis Title	Investigation of Local Raw Materials for the Production of Lithium-ion Battery Separators in Thailand
Author	Panalee Kerdthong
Degree	Master of Science (Materials Innovation for Sustainability)
Advisor	Assistant Professor Sitthi Duangphet, Ph. D.
Co-Advisor	Assistant Professor Uraiwan Intatha, Ph. D. Associate Professor Nattakan Soykeabkaew, Ph. D.

ABSTRACT

This study investigates the influence of die exit temperature on the crystalline structure, morphology, and electrochemical performance of polypropylene (PP) separators fabricated via the dry stretching process. The objective was to optimize processing conditions and evaluate the feasibility of using both imported (Sinopec PPH-T03-S) and domestic (IRPC S1003) polypropylene resins for lithium-ion battery separator production.

Precursor films were extruded at die exit temperatures ranging from 215 °C to 245 °C with a die draw ratio (DDR) of 160, followed by cold and hot stretching to generate microporous structures. Polarized FTIR and 2D-WAXS analyses indicated that lower die exit temperatures enhanced crystalline orientation and promoted well-aligned lamellae. SEM observations showed that separators fabricated at 215 °C exhibited elongated and interconnected pores, while higher temperatures resulted in distorted lamellae, non-uniform pores, and partial pore closure.

Electrochemical testing revealed that the separator produced at 215°C achieved the highest electrolyte uptake (109.4 ± 4.4%) and superior charge–discharge performance, delivering a specific discharge capacity of approximately 178 mAh/g with an efficiency of 98.5%. Separators prepared at 230°C and 245°C exhibited reduced ionic transport and lower capacity due to suppressed pore formation and partial pore collapse.

For the domestic IRPC S1003 resin, a similar temperature-dependent trend was observed. The separator fabricated at 215 °C showed balanced pore morphology and

competitive electrochemical performance, whereas higher die exit temperatures led to either limited ionic conductivity or structural instability.

The scalability of the optimized condition was further evaluated using a machine direction orientation (MDO) process. MDO-fabricated separators exhibited finer and more uniformly aligned pores, improved dimensional stability, and extended cycle life exceeding 50 cycles, with charge–discharge efficiencies approaching 99%.

Overall, a die exit temperature of 215 °C was identified as the optimal condition, and the results demonstrate that domestic polypropylene can be effectively utilized for scalable lithium-ion battery separator production through appropriate processing control.

Keywords: Lithium-ion Battery, Separator, Polypropylene, Dry Process, Die Exit Temperature, Scale-up

TABLE OF CONTENTS

TABLE OF CONTENTS (Continued)

LIST OF TABLES

LIST OF FIGURES

CHAPTER 1

INTRODUCTION

1.1 Research Background

Lithium-ion batteries (LIBs) have revolutionized the energy storage landscape, becoming the cornerstone of modern portable electronics, electric vehicles (EVs), and renewable energy systems (Goodenough & Park, 2013; Manthiram, 2020; Tarascon & Armand, 2001). Their high energy density, long cycle life, and relatively low self-discharge rate make them superior to other battery chemistries. However, the performance and safety of LIBs are not solely determined by the electrodes and electrolytes; the separator, a critical yet often overlooked component, plays a crucial role in the overall functionality and reliability of the battery (Arora & Zhang, 2004; Lee et al., 2014).

The general components of LIBs are shown in Figure 1.1 lithium-ion battery consists of an anode and a cathode that store and release lithium ions during charging and discharging. These electrodes are separated by a microporous separator, typically made of polypropylene, which prevents short circuits while allowing ions to pass through (Scrosati & Garche, 2010). The electrolyte, a liquid or gel with lithium salts in organic solvents, enables ion movement between the anode and cathode (Xu, 2014). Current collectors (copper for the anode and aluminum for the cathode) conduct electrons to and from the external circuit, ensuring efficient energy transfer, while all components are housed within a protective casing to maintain the battery’s integrity and safety (Zhang, 2007).

The separator in a lithium-ion battery is a pivotal component that significantly influences the battery's safety, performance, and longevity. Placed between the anode and cathode, the separator's primary role is to prevent direct physical contact between these electrodes, thus avoiding short circuits that could lead to battery failure or hazardous conditions (Arora & Zhang, 2004). Usually made from microporous membranes of polyolefin, the separator allows lithium ions to move freely through its

structure while maintaining electrical isolation between the anode and cathode (Deimede & Elmasides, 2015; Zhang, 2007). This ion flow is crucial for the battery's charge and discharge cycles, directly impacting its efficiency and capacity.

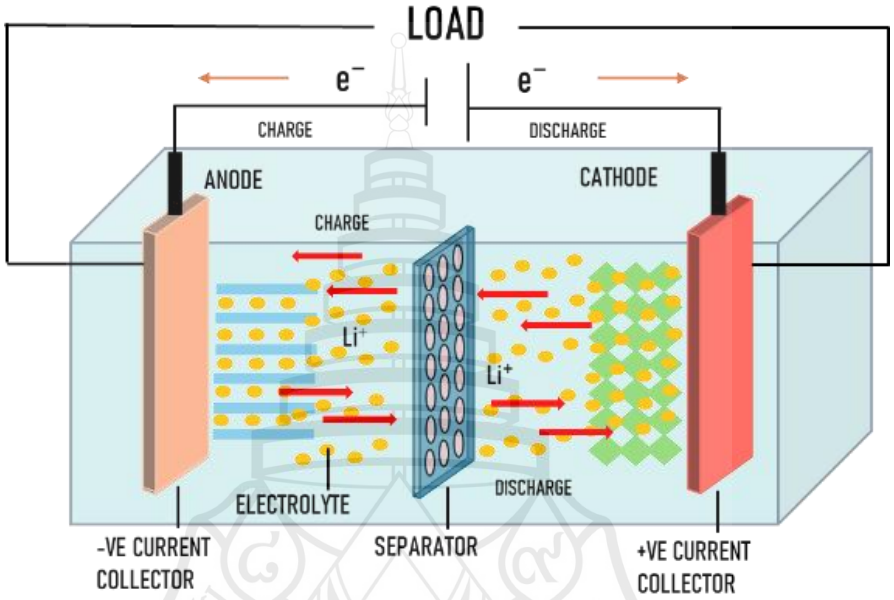

Source adapted from Lei & Xu (2017)

Figure 1.1 Lithium-ion battery components.

The performance of lithium-ion batteries, such as high energy density, long cycle life, and low self-discharge, depends heavily on the quality of the separator. A well-designed separator ensures efficient ionic conduction, mechanical stability, and thermal resistance, which are vital for reliable battery operation (Lee et al., 2014; Liu et al., 2018). As the demand for advanced lithium-ion batteries grows in areas such as portable electronics, electric vehicles (EVs), and renewable energy storage, optimizing separator materials and manufacturing processes becomes increasingly important (Yang & Hou, 2012).

There are primarily two methods for producing separators for lithium-ion batteries: the wet process and the dry process. The wet process involves coating a ceramic or polymer substrate with a slurry containing the desired separator material, followed by a drying process to remove the solvent. This method allows for precise control over separator thickness and porosity, making it suitable for producing

separators with uniform properties over large areas (Deimede & Elmasides, 2015). However, it requires the use of solvents, which can be environmentally harmful and increase production costs. Additionally, the complex processing steps involved may lead to inconsistent separator properties and batch-to-batch variations (Arora & Zhang, 2004).

On the other hand, the dry process involves melting extrusion and stretching of the separator material, usually polypropylene or polyethylene, to form a porous membrane without the need for solvents (Tabatabaei et al., 2009). This method offers several advantages, including environmental friendliness due to the absence of solvents, simplified processing steps leading to higher efficiency and scalability, and enhanced control over separator properties such as pore size distribution and mechanical strength (Xu et al., 2015). The dry process is favored over the wet process for its cost-effectiveness, consistent product quality, and alignment with sustainable manufacturing practices, making it the preferred method for producing separators for lithium-ion batteries. On the other hand, the dry process is suitable only for crystalline polymers such as polypropylene (PP) and polyethylene (PE), which excludes amorphous polymers that could otherwise offer advantages such as higher ionic conductivity and flexibility (Ding et al., 2019).

The lithium-ion battery assembly industry in Thailand is currently on the rise, attracting considerable attention. However, despite this growth, many essential components still need to be imported from abroad. IRPC Public Company Limited, a leading polypropylene producer with extensive expertise in forming polypropylene films, stands poised at the forefront of addressing this challenge. There is a pressing need to explore the possibility of IRPC becoming a producer or supplier of plastic pellets to manufacturers of membranes for lithium-ion batteries, particularly utilizing dry production methods from polypropylene. This collaboration marks the genesis of an exciting venture, promising to strengthen the local battery manufacturing landscape while capitalizing on IRPC's expertise and Thailand's growing industrial potential (Palacín, 2009).

1.2 Research Objectives

1.2.1 To study the processing parameters of membrane fabrication effect on LIBs quality. The parameters in this study consist of extrusion parameters (exit die temperature, air knife, first roll temperature and die draw ratio) and stretching parameters (cold stretching ratio and hot stretching ratio).

1.2.2 To compare the sources of Polypropylene (PP) raw materials on process feasibility.

1.3 Scope of Work

The scope of this work has been divided into three main steps, as described below.

1.3.1 Literature review and material selection

This step focuses on studying relevant literature related to lithium-ion battery separators, dry process fabrication, and polypropylene-based microporous membranes. Based on the literature review, a commercial polypropylene homopolymer from Sinopec was selected as the reference raw material due to its comprehensive and well-documented material parameters, including molecular weight, melt flow rate, and crystallinity. These properties serve as key indicators for separator fabrication and process optimization in the subsequent steps.

1.3.2 Membrane fabrication and characterization

This step investigates the fabrication of polypropylene separators using the dry production method and systematically studies the processing parameters affecting separator structure and performance. The fabrication process begins with precursor film preparation, in which a single-screw extruder is used to process polypropylene homopolymer into cast films. Key extrusion parameters studied in this step include die draw ratio, die exit temperature, air knife condition, and first chill roll temperature, all of which play a crucial role in determining crystalline orientation and film morphology.

After extrusion, the precursor films undergo annealing to promote an ordered crystalline arrangement and enhance lamellar stability prior to stretching.

Subsequently, cold stretching is performed at room temperature to initiate pore formation in the amorphous regions of the film, followed by hot stretching at elevated temperatures to enlarge and stabilize the pore structure. Finally, a heat-setting process is applied to balance polymer chain orientation and minimize thermal shrinkage after stretching.

Characterization in this step is divided into two main parts. The precursor films are characterized using polarized FTIR and two-dimensional wide-angle X-ray scattering (2D-WAXS) to evaluate crystalline orientation and structural development. After hot stretching, the separator membranes are characterized by scanning electron microscopy (SEM), pore size analysis, thickness measurement, electrolyte uptake, and thermal shrinkage evaluation.

The optimized Sinopec-based separator is then assembled into lithium-ion coin cells, and battery performance is evaluated through charge–discharge efficiency, specific capacity, and cycling stability tests.

Based on the optimized parameters obtained from Sinopec, a domestic polypropylene raw material (IRPC S1003) with properties closest to Sinopec, particularly molecular weight and crystallinity, is selected. Separators fabricated from IRPC S1003 are processed using the same dry production conditions, and their structural and electrochemical properties are characterized and evaluated in the same manner as those of the Sinopec-based separators.

1.3.3 Scale-Up production

This step investigates the feasibility of scaling up the separator fabrication process using the optimized parameters obtained from laboratory-scale experiments. Instead of using a uniaxial tensile machine (UTM) for stretching, a machine direction orientation (MDO) system is employed to simulate industrial-scale production conditions.

In this step, hot and cold stretching are conducted using the MDO machine, and the resulting separator membranes are characterized to assess pore morphology, dimensional stability, and electrolyte uptake. The electrochemical performance of MDO-fabricated separators is also evaluated and compared with laboratory-scale results to determine the scalability and industrial potential of the proposed dry production process.

CHAPTER 2

LITERATURE REVIEW

2.1 Requirements for Separators

There are several factors to consider when selecting a separator for use in a lithium-ion battery, as summarized in Table 2.1.

Table 2.1 Basic properties of separators.

Parameter	Requirement
Chemical and electrochemical stabilities	Stable for a long period of time
Wettability	Wet out quickly and completely
Mechanical property	>1000 kg cm^{-1} (98.06 MPa)
Thickness	20-25 0.1 μm
Pore size	<1 μm
Porosity	40–60%
Permeability (Gurley)	<0.025 s μm^{-1}
Dimensional stability	No curl up and lay flat
Thermal stability	<5% shrinkage after 60 min at 90 °C
Shutdown	Effectively shut down the battery at elevated temperatures

Source Lee et al. (2014)

2.1.1 Chemical stability

The primary property of a separator in lithium-ion batteries is its chemical and electrochemical stability against the electrolyte and electrode materials. The membrane must exhibit robust chemical stability to resist degradation or mechanical loss resulting from reactions or decomposition processes. Additionally, the electrolyte should not undergo adverse reactions, particularly under oxidizing conditions, which are prevalent during battery charging and discharging cycles (Arora & Zhang, 2004; Zhang, 2007).

Any chemical changes in the electrolyte could compromise battery performance and safety. Furthermore, the separator must not generate impurities that could interfere with the battery's operation. Ensuring these stability criteria are met is essential for maintaining the integrity and functionality of lithium-ion batteries throughout their operational lifespan.

2.1.2 Wettability

Wettability is indeed a crucial property for separators in lithium-ion batteries due to their interaction with electrolytes. Electrolytes play a vital role in ion transport within the battery. A permeable membrane must absorb and retain a certain amount of electrolyte fluid to maintain low internal resistance and high ionic conductivity. Moreover, the membrane should have the ability to rapidly absorb electrolyte liquid, reducing the time required for electrolyte addition during battery assembly. The speed of electrolyte adsorption is influenced by various factors, including the type of polymer used in the membrane, its porosity, pore size, and the tortuosity of the structure. Optimizing these parameters can enhance the membrane's wettability and ensure efficient electrolyte absorption, thereby improving battery performance and assembly efficiency (Arora & Zhang, 2004; Huang, 2011; Lee et al., 2014; Zhang, 2007).

2.1.3 Thickness

The thickness of membranes used in rechargeable batteries typically falls within the range of 20–25 μm (Palacín, 2009). This thickness balance aims to achieve low internal resistance and high-power output while maintaining high energy density. However, opting for thinner membranes may compromise mechanical properties, increasing the risk of tearing during battery assembly and potentially resulting in short circuits. Therefore, selecting a thicker and more separators can mitigate this risk. Additionally, ensuring thickness uniformity across the membrane is crucial for maintaining battery stability and extending its lifespan. Achieving these balance and uniformity considerations in membrane thickness contributes significantly to the overall performance and safety of lithium-ion batteries.

2.1.4 Porosity

The permeable membrane in lithium-ion batteries must possess appropriate porosity to effectively retain electrolyte content within its pores, thereby maintaining high ionic conductivity. Typically, the permeable membrane used in these batteries has

a porosity of approximately 40 percent (Arora & Zhang, 2004). If the porosity is too low, internal resistance may increase due to insufficient electrolyte content. Conversely, excessively high porosity levels can compromise mechanical properties and lead to safety issues. High porosity also affects the membrane's ability to close pores during thermal shutdown events, where excessive heat may cause pores to remain open, potentially resulting in short circuits. Thus, achieving an optimal balance in porosity is critical for ensuring both efficient ion transport and battery safety in lithium-ion applications.

2.1.5 Pore size and pore distribution

The pore size of the separator in lithium-ion batteries must be smaller than the particle size of the electrode assembly to prevent short circuits. Submicron pore sizes, typically less than 1 μm, are considered ideal for these membranes. Such small pore sizes effectively block particle penetration from electrode components or dendritic lithium metal branches that may form during battery operation, stability of thus minimizing the risk of short circuits (Deimede & Elmasides, 2015).

Additionally, ensuring uniformity in pore size distribution is crucial. An uneven distribution can lead to efficiency loss due to non-uniform current distribution within the battery. Therefore, maintaining consistent and uniform pore sizes across the membrane is essential for optimizing battery performance and reliability.

2.1.6 Permeability

An essential property of a separator is its permeability, which refers to its ability to allow the passage of ions while resisting the flow of solid components. Increasing the solid content of a permeable membrane can elevate the resistance of the ion-conducting electrolyte, affecting its permeability. Permeability is often quantified using the MacMullin number (Abraham, 1993), which represents the ratio of the resistance of a membrane soaked in a liquid electrolyte to the resistance of the electrolyte alone. This number can be estimated from the air permeability of the membrane, expressed as the Gurley value (Arora & Zhang, 2004). The Gurley value is determined by measuring the time required for a specific volume of air to permeate a known area of the membrane under a given pressure. A low Gurley value indicates high porosity and low tortuosity of the permeable membrane, indicative of superior permeability. For membranes used in lithium-ion batteries, the optimum Gurley value is typically less than 0.025 s μm-1,

as measured by the ASTM D726 method. Achieving this optimal Gurley value ensures efficient ion transport and optimal battery performance.

2.1.7 Dimensional stability

Dimensional stability is a crucial property for permeable membranes in lithium-ion batteries, ensuring they remain flat and do not curl when impregnated with liquid electrolyte. Curling or buckling can lead to misalignment between the membrane and the electrodes during battery assembly (Arora & Zhang, 2004), potentially compromising battery performance and safety. Additionally, the membrane should maintain a constant size throughout battery storage and operating conditions, especially in applications with wide temperature ranges. Fluctuations in temperature can cause expansion or contraction of the membrane, which may affect its performance and the overall functionality of the battery. Therefore, achieving dimensional stability is essential for ensuring the reliable operation of lithium-ion batteries in various environmental conditions.

2.1.8 Thermal shrinkage

Thermal shrinkage is another critical consideration for separators in lithium-ion batteries. The membrane should resist noticeable shrinking and wrinkling as the temperature increases, particularly during the drying process in battery assembly. Excessive thermal shrinkage can lead to dimensional changes in the membrane, affecting its fit and alignment within the battery cell. To ensure stability and reliability, thermal shrinkage should be minimized, with a maximum allowable shrinkage of 5 percent after heating at 90 degrees Celsius for 60 minutes (Deimede & Elmasides, 2015). By maintaining dimensional stability under thermal stress, the separator can contribute to the overall performance and safety of lithium-ion batteries across a range of operating conditions.

2.1.9 Electrolyte uptake

Electrolyte uptake is a critical property of lithium-ion battery separators, directly influencing the battery's ionic conductivity, internal resistance, and overall performance. The mechanism of electrolyte uptake involves several key factors: porosity, which determines the volume of electrolyte the separator can hold; pore size and distribution, ensuring quick and uniform absorption while preventing dendrite growth and particle penetration; and surface chemistry (Zhang et al., 2015), where

hydrophilic surfaces enhance wettability and absorption. The polymer type, such as polyethylene (PE) and polypropylene (PP), affects compatibility with the electrolyte, with surface treatments improving hydrophobic polymers' affinity for electrolytes. Additionally, the thickness of the separator must balance electrolyte capacity with mechanical strength to optimize performance. The absorption rate is crucial during battery assembly, where rapid uptake reduces electrolyte filling time. Overall, optimizing these factors ensures efficient electrolyte uptake, maintaining low internal resistance and high ionic conductivity, essential for the battery's performance and longevity.

2.2 The Production Process of Separator for Lithium-ion Batteries

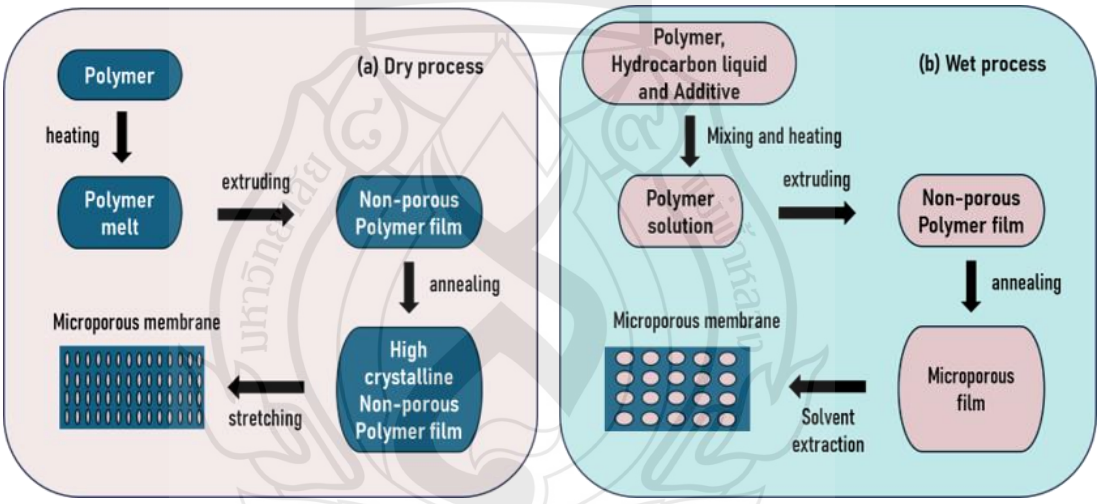

Source Deimede & Elmasides (2015)

Figure 2.1 Processing of lithium-ion battery separator (a) Dry process and (b) Wet process.

The production processes of separators for lithium-ion batteries encompass a wide range of methods and materials, which can be broadly classified into four main types: microporous membranes, nonwoven mats, composite membranes, and polymer gels. Each category employs distinct fabrication techniques to achieve specific membrane characteristics suitable for battery applications, such as ionic conductivity, mechanical strength, and thermal stability. Common processing methods include dry

processing, wet processing, phase inversion, electrospinning, and related techniques (Deimede & Elmasides, 2015).

Among these types, microporous membranes are the most widely used in large-scale commercial lithium-ion battery production due to their versatility and compatibility with both dry and wet processing routes. As illustrated in Figure 2.1 microporous membrane fabrication typically involves a two-step manufacturing approach, beginning with polymer extrusion or film casting to form a dense precursor film, followed by a stretching process to induce porosity within the membrane structure.

Dry-processed separators are particularly suitable for lithium-ion batteries that prioritize high energy density. This suitability arises from their open, straight, and highly oriented pore structure, which facilitates efficient lithium-ion transport and minimizes internal resistance within the battery. In contrast, wet-processed separators are often preferred for applications requiring enhanced cycle life, as their interconnected and tortuous pore networks are more effective in suppressing lithium dendrite growth during repeated charging and discharging cycles (Lee et al., 2014).

The dry process consists of several essential steps, as shown schematically in Figure 2.1(a), including extrusion, annealing, stretching, and relaxation. Initially, polymer extrusion produces a dense precursor film without porosity but with lamellae arranged preferentially along the machine direction. During the subsequent annealing process, crystalline rearrangement occurs, enhancing lamellar regularity and increasing both the size and number of crystalline regions, which are critical for controlled pore development during stretching.

Following annealing, the precursor film is stretched along the same direction as extrusion. Cold stretching is first applied to initiate micropores within the amorphous regions of the polymer matrix. This step is followed by hot stretching, which enlarges and stabilizes the pore structure by further separating the lamellae. Finally, a relaxation or heat-setting process is conducted to relieve internal stresses and improve dimensional stability of the dry-processed membrane (Chandavasu et al., 2000; Johnson & Wilkes, 2002).

The pore structure of dry-processed membranes is influenced by several factors, including the morphological characteristics of the precursor film, annealing conditions, and stretching parameters. Key variables include annealing temperature and duration,

draw ratio, pulling speed, and stretching temperature, all of which play critical roles in determining pore size, orientation, and uniformity.

Dry processing offers significant advantages over wet processing due to the absence of organic solvents, resulting in a more environmentally friendly and cost-effective manufacturing route. However, this method is limited to semi-crystalline polymers, particularly polyethylene (PE) and polypropylene (PP), as pore formation relies on lamellar separation during stretching (Deimede & Elmasides, 2015). Commercial examples of dry-processed separators include products from Celgard (Polypore) (Arora & Zhang, 2004; Zhang, 2007) and UBE Industries Ltd. (Zhang, 2007).

In contrast to dry processing, wet processing produces membranes with pores that are generally elliptical, less oriented, and highly interconnected, as illustrated in Figure 2.2(b). These pore characteristics arise because porosity is generated primarily through solvent and additive extraction rather than mechanical stretching. The interconnected pore network enhances electrolyte retention and contributes to improved cycling stability, although ionic transport resistance may be higher compared to dry-processed membranes.

As shown in Figure 2.1(b), wet processing typically involves mixing polymers with additives or plasticizers and hydrocarbon liquids, followed by heating and extrusion to form a non-porous film. Subsequently, selective extraction of the liquid phase and additives using volatile solvents creates a microporous structure (Arora & Zhang, 2004; Deimede & Elmasides, 2015). Stretching may be applied either before or during solvent extraction and can be performed uniaxially or biaxially to control pore size and distribution.

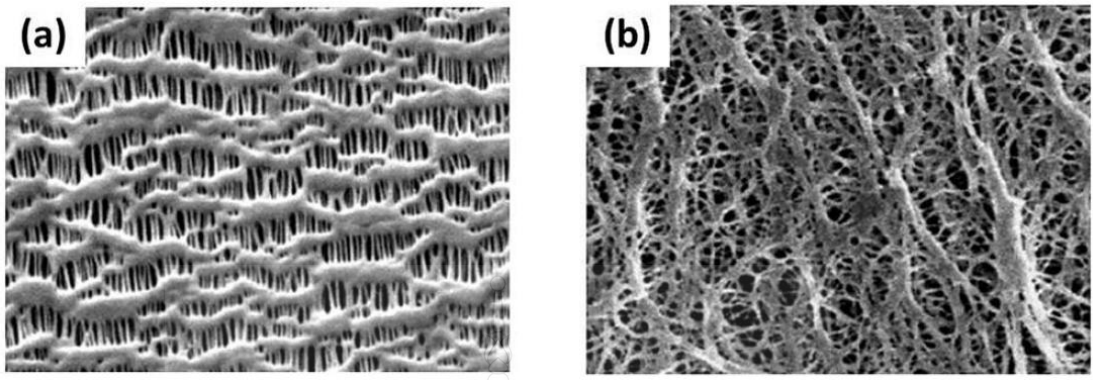

Source Xu et al. (2018)

Figure 2.2 SEM image of separator by (a) dry process and (b) wet process

The pore structure of wet-processed membranes is strongly influenced by polymer composition, the type and concentration of additives and solvents, and stretching conditions. Unlike the dry process, wet processing is compatible with a broader range of polymers, including both semi-crystalline and amorphous materials. However, the need for solvent extraction and, in many cases, biaxial stretching increases production complexity and cost.

Well-known manufacturers of wet-processed lithium-ion battery separators include Asahi Kasei, Toray Industries, Mitsui Chemicals, and Entek (Deimede & Elmasides, 2015). These membranes are widely employed in applications that demand long cycle life and enhanced safety due to their stable and interconnected pore structures.

2.3 Manufacturing of Lithium-ion Battery Separator of PP by Dry Process

Each process of the dry process consists of the following important steps: (1) Precursor film extrusion (2) Annealing (3) Cold stretching (4) Hot stretching (5) Heat setting. Each sub-process is important to the quality of the separator. The crystallization development and pore formation during each steps depict in Figure 2.3

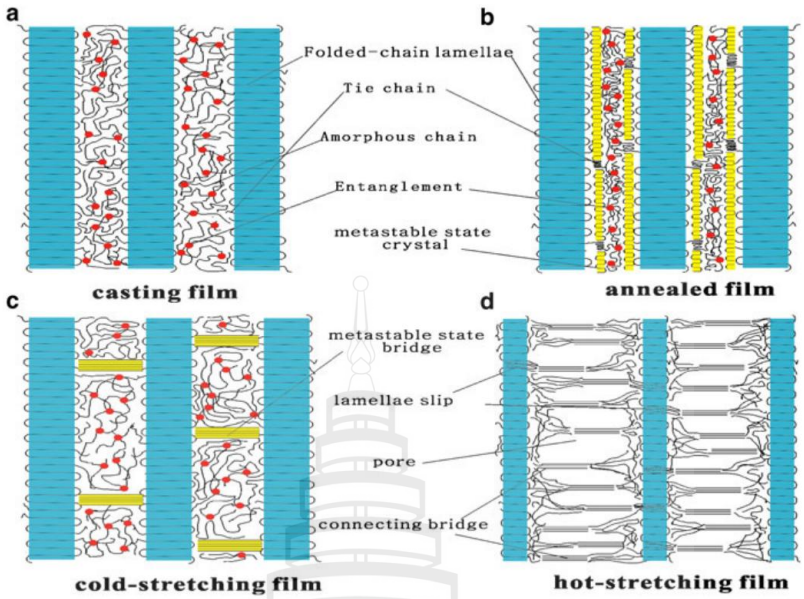

Source Lei & Xu (2017)

Figure 2.3 Connecting bridges formation process during stretching.

2.3.1 Precursor film extrusion

This is an important process that controls the PP crystals to have an appropriate arrangement for the subsequent separator manufacturing process. the polymer resins are melted-extruded to form a uniaxially oriented tubular film, referred to as the precursor film. The morphology and orientation of this film are determined by the processing conditions and the properties of the polymer resins. Typically, the film must possess a crystalline row structure, with lamellae arranged in rows and their long axes perpendicular to the machine direction (MD). This arrangement is essential for the creation of micropores, as only the stacked lamellae can "open" during the subsequent stretching process (Zhang, 2007).

2.3.1.1 Effect of die draw ratio (DDR) on separators

Die draw ratio (DDR) significantly affects the properties of lithium-ion battery separators through a detailed mechanism involving the stretching and alignment of polymer chains during the extrusion process. Die draw ratio (DDR) is defined as the ratio of the take-up speed to the average velocity of the polymer melt at the die exit, and it is widely used to indicate the degree of stretching imposed along the machine direction during precursor film extrusion (R. Xu et al., 2015), and it determines the

extent to which the polymer material is stretched. As shown in Figure 2.4(b), a higher DDR results in a greater degree of polymer chain stretching and alignment along the machine direction. This enhanced molecular orientation promotes the formation of a more ordered crystalline row structure in the precursor film, which facilitates controlled lamellar separation during subsequent stretching (Tabatabaei et al., 2009; R. Xu et al., 2015). As a result, the separator exhibits a more uniform and well-distributed microporous morphology. Such pore structures are advantageous for lithium-ion battery performance, as they enhance electrolyte uptake and retention, leading to improved ionic conductivity and reduced internal resistance during battery operation (Sadeghi et al., 2007b; Tabatabaei et al., 2009). In addition, the increased chain alignment associated with high DDR contributes to improved mechanical strength and thermal stability, enhancing the separator's resistance to tearing and deformation during battery assembly and cycling.

Conversely, Figure 2.4(a) the separator produced from precursor film extruded at lower DDR results in less orientation of the polymer chains, leading to weaker mechanical properties, irregular and less uniform pore structures, and higher internal resistance due to inefficient ion transport pathways. Therefore, optimizing the DDR is critical in the production of high-performance (Lei et al., 2013), reliable separators for lithium-ion batteries.

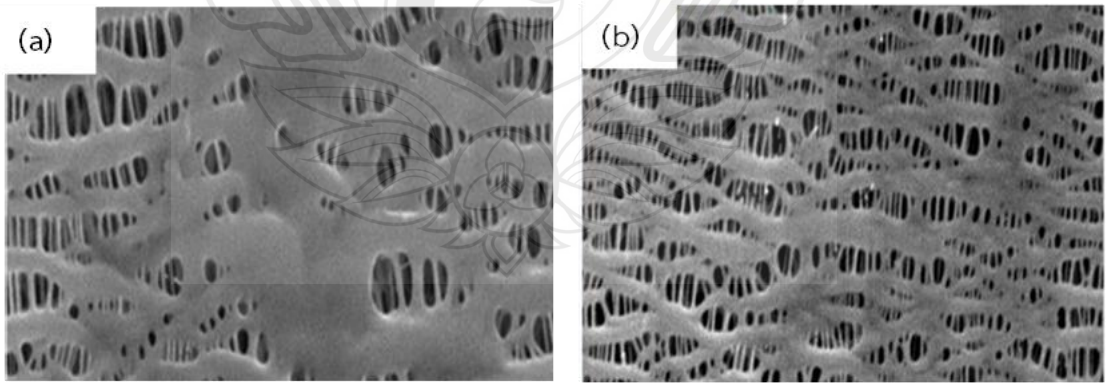

Source Xu et al. (2015)

Figure 2.4 SEM image of separator prepared from precursor film extruded at different DDR and stretched at room temperature to 25% and then at 130 °C to 100%. (a) 80DDR (b) 160DDR.

2.3.1.2 Effect of air knife on separators

The use of an air knife in the production of lithium-ion battery separators plays a crucial role in defining the final properties of the separator by influencing the cooling and solidification process of the extruded polymer film (Cai et al., 2016; Ren et al., 2018). The air knife, a high-velocity air stream, is applied to the extruded film immediately after it exits the die, controlling the cooling rate and solidifying the film surface. The mechanism involves rapid cooling, which helps in achieving a fine, desired mechanical properties and uniform pore structure as seen in Figure 2.5. When the high-velocity air from the air knife hits the hot, extruded film, it causes an immediate drop in temperature on the film surface, leading to rapid solidification of the outer layer while the inner layers are still molten. This creates a skin-core structure where the outer skin becomes more crystalline and oriented, enhancing the mechanical strength and thermal (Lee et al., 2014).

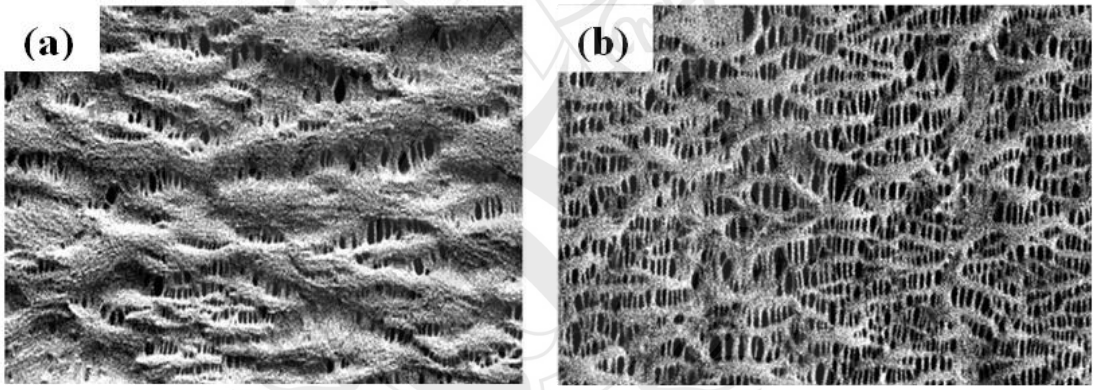

Source Tabatabaei et al. (2009)

Figure 2.5 SEM image of separator prepared from precursor film (a) non-air knife (b) with Air knife.

Furthermore, the air knife influences the porosity and pore size distribution of the separator. The rapid cooling effect can induce phase separation in the polymer, contributing to the formation of a microporous structure with controlled pore size and uniform distribution (Tabatabaei et al., 2009). This is essential for maintaining low internal resistance and high ionic conductivity within the battery, as a well-defined pore structure facilitates efficient electrolyte absorption and retention. Controlled cooling

also minimizes the risk of defects such as voids or uneven thickness (Arora & Zhang, 2004), which can compromise the separator's performance and safety.

Additionally, the air knife parameters, including air velocity, air temperature, and positioning, can be adjusted to control the cooling behavior of the extruded film. Higher air velocity and lower air temperature increase the cooling rate, which promotes faster surface solidification and can influence the development of the precursor film structure (Sadeghi et al., 2007b). In contrast, lower air velocity and higher air temperature result in slower cooling, leading to different pore evolution and mechanical behavior after subsequent stretching. Therefore, proper control of air knife operating conditions is an important factor in achieving stable processing and consistent separator properties for lithium-ion batteries.

2.3.1.3 Effect of first roll temperature on separator

The first roll temperature in the manufacturing process of lithium-ion battery separators plays a crucial role in defining the final properties of the separator. During the extrusion and stretching stages, the polymer film is passed over a series of heated rolls, with the first roll temperature being particularly important. This initial temperature affects the crystalline and molecular orientation of the polymer chains (Sadeghi et al., 2007b). At an optimal first roll temperature, the polymer chains begin to orient and crystallize properly, which contributes to the formation of a uniform film with enhanced mechanical strength and structural stability, facilitating the development of the desired microporous structure. If the temperature is too low, the polymer may not achieve sufficient mobility, leading to inadequate stretching and poor pore formation. Conversely, if the temperature is too high, excessive chain mobility may occur, resulting in less controlled pore evolution and possible thermal degradation of the polymer (Mun & Won, 2021; Sadeghi et al., 2007b).

Additionally, the first roll temperature impacts the thermal shrinkage behavior and dimensional stability of the separator (Mun & Won, 2021). Properly controlled temperatures ensure that the film does not shrink or wrinkle during subsequent processing and battery operation. Therefore, the first roll temperature must be precisely controlled to balance these factors, ensuring the separator has the necessary mechanical strength, thermal stability, and electrochemical performance for efficient battery operation.

2.3.2 Annealing

Annealing is a critical process in the production of lithium-ion battery separators, significantly influencing their properties through a mechanism that involves controlled heating and cooling. During annealing, the film is heated to a temperature below its melting point, allowing the polymer chains to reorient and recrystallize. This controlled thermal treatment enhances the crystalline structure of the polymer, improving mechanical strength, thermal stability, and dimensional stability (Wang et al., 2015).

At an optimal annealing temperature, the polymer chains gain sufficient mobility to align and form more ordered crystalline regions. This increased crystallinity reduces the separator's porosity, leading to a more uniform microporous structure essential for effective ion transport. Enhanced crystallinity also contributes to improved mechanical integrity, increasing resistance to deformation and tearing during battery assembly and operation (Liu et al., 2019; Wang et al., 2015).

Furthermore, annealing helps in relieving internal stresses generated during the extrusion and stretching processes, thus minimizing shrinkage and warping. This stress relief is crucial for maintaining the separator's dimensional stability and ensuring consistent performance over the battery's lifespan (Liu et al., 2019).

Precise control of annealing temperature and duration is important for achieving appropriate crystalline reorganization in the precursor film. Insufficient annealing may leave residual stresses and incomplete crystal development, whereas excessive annealing can promote thermal degradation or excessive crystal growth. Therefore, optimization of annealing conditions is necessary to obtain a stable crystalline structure prior to the stretching process (Cai et al., 2016; Lei et al., 2013; Liu et al., 2019).

2.3.3 Cold stretching

Cold stretching is a crucial process in the production of lithium-ion battery separators, significantly impacting their properties through a detailed mechanism. This process involves elongating the polymer film at temperatures below its melting point, which induces a controlled deformation of the polymer chains. During cold stretching, the polymer chains are oriented in the direction of the stretch, which enhances the mechanical properties of the separator, such as tensile strength and dimensional stability (Tabatabaei et al., 2009).

The cold stretching process begins by initially cooling the extruded polymer film to a temperature where it becomes less flexible but still deformable. This cooling ensures that the polymer chains are in a semi-crystalline state, which is ideal for creating a uniform microporous structure. As the film is stretched, the crystalline regions are elongated and aligned, while the amorphous regions become more ordered. This alignment and elongation process helps to create interconnected pores that are essential for efficient ion transport within the batter (Lei & Xu, 2017).

Moreover, cold stretching affects the pore size and distribution within the separator. By controlling the degree of stretching, manufacturers can fine-tune the pore structure to achieve the desired balance between mechanical strength and ionic conductivity. A well-optimized cold stretching process ensures that the separator has a uniform and interconnected pore network, which facilitates efficient electrolyte absorption and retention, thereby enhancing the overall performance of the lithium-ion battery (Lei et al., 2018).

2.3.4 Hot stretching

Hot stretching is performed to enlarge and stabilize the microporous structure formed during the previous processing steps. This process is conducted at temperatures above the glass transition temperature (Tg) but below the melting temperature (Tm), allowing increased mobility of the polymer chains without destroying the crystalline framework.

At this temperature range, polymer chains in the amorphous regions gain sufficient mobility to rearrange, while the crystalline regions remain intact and become further oriented along the stretching direction. This results in extended and better-aligned crystalline lamellae, while maintaining structural continuity within the film (Cai et al., 2016; Lei et al., 2013).

In addition to molecular reorganization, hot stretching promotes the expansion and interconnection of pores initially generated during cold stretching. The increased chain mobility allows controlled separation between lamellae, leading to a more continuous pore network. Such structural development improves electrolyte infiltration and reduces ionic transport resistance within the separator (Xu et al., 2018; Saffar et al., 2014).

2.3.5 Heat setting

Heat setting is a crucial step in the production of lithium-ion battery separators, impacting their thermal and mechanical properties through a detailed mechanism. This process involves heating the stretched polymer film to a specific temperature below its melting point and maintaining it for a set period. During heat setting, the polymer chains relax and rearrange into a more thermodynamically stable configuration, enhancing the crystallinity and uniformity of the film (Arora & Zhang, 2004).

The primary mechanism involves the relaxation of internal stresses induced during stretching. As the film is heated, the polymer chains gain mobility, allowing them to adjust and align into a more ordered crystalline structure. This reorganization reduces internal stress, leading to improved dimensional stability and mechanical integrity (Tabatabaei et al., 2009). The increased crystallinity enhances the film's thermal stability, making it more resistant to shrinkage and deformation under high temperatures encountered during battery operation (Xu et al., 2018).

Heat setting also affects the microporous structure of the separator. The controlled heating process helps to stabilize the pore size and distribution formed during stretching, ensuring that the pores remain well-defined and interconnected. This is crucial for maintaining high ionic conductivity and low internal resistance in the battery, as it facilitates efficient electrolyte absorption and retention. The uniform pore structure also contributes to the mechanical strength of the separator, preventing defects that could lead to short circuits or other failures (Xu et al., 2018).

2.4 Effect of Chemical Structure of PP on Separator

The chemical structure of polypropylene (PP) significantly influences the performance of lithium-ion battery separators. The arrangement of polymer chains, tacticity (isotactic, syndiotactic, or atactic), and degree of crystallinity directly affect the mechanical strength, thermal stability, and electrolyte uptake of the separator. Isotactic PP, with its highly regular structure, offers higher crystallinity and mechanical strength, which are crucial for the separator's durability and performance (Ikezaki et al.,

1981). In contrast, atactic PP, with its irregular structure, tends to have lower crystallinity and weaker mechanical properties.

2.4.1 Molecular weight

The molecular weight (Mw) of polypropylene (PP) in lithium-ion battery separators significantly impacts their properties, with two key aspects being chain length and molecular weight distribution. Understanding the mechanisms underlying these factors is crucial for tailoring separator properties to enhance battery performance and safety.

2.4.1.1 Chain length

The chain length of polypropylene molecules directly affects the separator's mechanical properties and electrolyte transport characteristics. Longer polymer chains, corresponding to higher molecular weights, result in more entangled structures within the separator membrane. This increased chain entanglement enhances mechanical strength, making the separator more resistant to punctures or tears during battery manufacturing, assembly, and operation. Moreover, longer polymer chains provide a larger surface area for electrolyte absorption, promoting efficient ion transport within the battery cell and facilitating electrochemical reactions. As a result, separators with higher molecular weight polypropylene tend to exhibit improved mechanical integrity and enhanced electrolyte uptake capacity, contributing to overall battery performance and longevity (Tabatabaei et al., 2009).

2.4.1.2 Molecular weight distribution

The molecular weight distribution (Mw distribution) of polypropylene influences the uniformity and consistency of separator properties. A narrow Mw distribution implies that most polymer chains have similar lengths, resulting in more uniform separator characteristics. In contrast, a broader Mw distribution indicates a wider range of chain lengths, leading to greater heterogeneity in separator properties. For instance, separators with a narrow Mw distribution typically exhibit more consistent pore sizes and porosity levels, facilitating uniform electrolyte distribution and ion transport throughout the battery cell. Conversely, separators with a broader Mw distribution may experience variations in pore size and porosity, which can affect ion diffusion rates and compromise battery performance. Therefore, controlling the Mw distribution of polypropylene is essential for ensuring the reproducibility and reliability

of separator properties, ultimately influencing battery efficiency and safety (Xu et al., 2014).

2.4.2 Branching

The presence of branching can disrupt the regular packing of polymer chains, leading to changes in the material's crystallinity and overall strength. Generally, increased branching tends to decrease the crystallinity of the polymer, resulting in a more amorphous structure with lower mechanical strength. This can impact the durability and puncture resistance of the separator, potentially compromising its ability to withstand mechanical stresses during battery assembly and operation.

Furthermore, branching influences the thermal stability of PP separators. Introducing branching can lower the melting point and thermal degradation temperature of the polymer, making it more susceptible to heat-induced degradation. This is particularly relevant in lithium-ion batteries, where separators may be exposed to elevated temperatures during manufacturing processes or under abusive conditions. Reduced thermal stability due to branching can lead to premature degradation of the separator material, affecting battery performance and safety (Sadeghi et al., 2007a; Tabatabaei et al., 2009b).

Additionally, branching can affect the porosity and pore structure of PP separators, which play critical roles in facilitating electrolyte transport and ion diffusion within the battery cell. Excessive branching may hinder the formation of well-defined pores, leading to decreased electrolyte uptake and slower ion transport kinetics. This can result in reduced battery efficiency and capacity, as well as increased internal resistance.

CHAPTER 3

EXPERIMENTAL

3.1 Materials

Commercial grade of Polypropylene was purchased from Sinopec, China (PPH-T03-S) with a density of 0.905 g/cm^{-3} (under ASTM D 792). The melt flow rate of 2.46 g/10min (under ASTM D 1238) condition of 230 ℃ and 2.16 kg. The melting point (Tm) obtained from DSC (Model Q2000 TA Instrument) at rate of 10 ℃/min, was 166.1 ℃. The molecular weight measured using GPC-IR Polymer Char's was 374,500 g/mol. The crystallinity was 49.4%.

IRPC Polypropylene S1003, Thailand with a density of 0.900 g/cm^{-3}. The melt flow rate of 3.41 g/10min condition of 230℃ and 2.16 kg. The melting point (Tm) obtained from DSC at rate of 10 ℃/min, was 167.59 ℃. The molecular weight was 365,800 g/mol. The crystallinity was 52.87%.

3.2 Preparation of Precursor Films

The precursor films were prepared by using single screw extruder (Collin Compounder ZK 25 E, Germany). The temperature profile begins from room temperature at hopper and increase to 245 ℃ at final zone before die exit. The die exit design was a coat-hanger die with 29 cm width and an average die gap was 1.76 mm. The extrusion die temperature was varied between 215 – 245 ℃. Distance between die exit to chill roll (Collin Chill-Roll 144/350, Germany) was set at 15 cm with apply an air knife (Chareontut Co. Ltd., Thailand). The first roll temperature of chill roll was varied between 80-90 ℃ and the speed of the first roll was varied to match the DDR between 80-180.Then the precursor films were collected and annealed in the oven at 145 ℃ for 30 minutes.

3.3 Preparation of Microporous Membranes

The annealed films were cut into specimens with dimensions of 25 mm in the transverse direction (CD) and 100 mm in the machine direction (MD). Uniaxial stretching was performed using a universal testing machine (Instron 5566, USA), with an initial gauge length of 50 mm, which was controlled by adjusting the distance between the grips.

Cold stretching was carried out along the machine direction (MD) at room temperature, with a strain of 15–25% at a stretching rate of 50 mm/min. Subsequently, hot stretching was conducted in a temperature-controlled chamber (Instron, USA) at 130 °C, with a strain of 80–100% at the same stretching rate.

Finally, the stretched films were subjected to heat setting at 145 °C for 10 min.

3.4 Scale-up Production of Polypropylene Separator

For scale-up production, the optimized processing conditions obtained from laboratory-scale stretching were applied to a machine-direction orientation (MDO) machine (Labtech Engineering Co., Ltd., Thailand). The annealed polypropylene precursor films were continuously fed into the MDO system and stretched along the machine direction (MD).

Cold stretching was first carried out at room temperature using a stretching ratio equivalent to a strain of 20%. Subsequently, hot stretching was performed in the heated stretching section of the MDO line at 130 °C using a stretching ratio equivalent to a strain of 100%. The stretching ratios were controlled by adjusting the speed difference between adjacent rolls. Finally, the stretched films were heat-set at 145 °C for 10 min.

3.5 Characterizations

3.4.1 Fourier Transform Infrared Spectroscopy (FTIR) and Polarized FTIR

For the measurements of crystal orientation, FTIR Microspectroscope (Bruker Tensor 27 Infrared Spectrometer connected to a Bruker Hyperion 3000 Infrared Microscope, Germany) was conducted using an appropriate instrument capable of

polarization. The sample was placed in the path of the polarized beam, and spectra were collected for both parallel and perpendicular polarizations relative to the melt extrusion direction. The results were analyzed using the OPUS 7.5 software (Bruker Optic Ltd, Ettlingen, Germany). The resulting data allowed for the calculation of the crystalline orientation factor *(Fc)*, which provides insights into how well-aligned the polymer chains are within the film. This characterization is essential for understanding and optimizing the material properties of the battery separator (Tabatabaei et al., 2009)

The dichroic ratio, *D*, is defined by the proportion of $A_{\parallel}$ & $A_{\perp}$ two absorption values following Equation (1):

$$D = \frac{A_{\parallel}}{A_{\perp}}$$

Where $A_{\parallel}$ represents the absorption parallel and $A_{\parallel}$ the absorption perpendicular to a specific reference axis, the Herman orientation function for this vibration is calculated according to Equation (2): (Sadeghi et al., 2007a).

$$f = \frac{D-1}{D+2}$$

For polypropylene two specific wave numbers were focused, absorption at a wavenumber of 998 cm^{-1} is associated with the crystalline phase (c-axis), while absorption at 972 cm^{-1} involves both crystalline and amorphous phases. From the former absorption, the crystalline phase orientation (f_c) can be determined, whereas the latter provides the average orientation function (f_{av}). The orientation of the amorphous phase (f_{am}) can then be calculated based on these values.

$$f_{av} = X_c f_c + (1 - X_c) f_{am}$$

where X_C represents the degree of crystallinity.

3.4.2 Two-dimensional wide-angle X-ray scattering (2D-WAXS)

Two-dimensional Wide-angle X-ray Scattering (2D-WAXS) is a technique used to investigate the crystalline structure and orientation of materials at the atomic and molecular levels. The 2D WAXS was operated at Synchrotron Light Research Institute,

Thailand using Beamline 1.3W equipped with SX165 CCD detector. The data was collected with X-ray energy 9 keV and accumulated 300 sec.

3.4.3 Scanning Electron Microscopy (SEM) and Pore Size Analysis

Scanning electron microscopy (SEM) (Tescan Mira, Czech Republic) was used to visualize the surface morphology and microstructure of the separators. A focused electron beam was scanned over the sample surface at an accelerating voltage of 5 keV. Prior to observation, the samples were coated with a thin layer of gold to enhance conductivity.

The pore size of the polypropylene microporous membranes was determined using ImageJ software. SEM images of the separators were captured and subsequently processed to quantify pore size and pore size distribution.

3.4.4 Electrolyte Uptake

The activated polymer electrolyte membrane was prepared by immersing the porous membranes in a battery-grade liquid electrolyte solution consisting of 1.0 M LiPF6 in EC/DEC (50:50 v/v) for 2 hours. The electrolyte uptake of the separator was calculated using Equation (3), where W_1 and W_2 denote the weights of the wet and dry membranes, respectively (Cui et al., 2017).

$$Uptake\ \% = \frac{W_2 - W_1}{W_1}\ x\ 100$$

3.4.5 Shrinkage

To evaluate the thermal shrinkage behavior, the separator was heated in an oven at 90°C for 1 hour. Thermal shrinkage was determined using Equation (4).

$$Shrinkage\ \% = \frac{S_0 - S_1}{S_0}\ x\ 100$$

Where S_1 and S_0 represent the separator's area after and before thermal treatment, respectively (Li et al., 2018).

3.4.6 Battery Performance

The electrochemical performance of lithium-ion batteries was evaluated using a Neware BST4000 battery testing system with BTS 7.6.x software (Neware, China). The system provided precise control and monitoring of charge–discharge processes under defined operating conditions.

Coin-type cells (CR2032 half-cells) were assembled and subjected to galvanostatic charge–discharge testing within a voltage window of 3.0–4.2 V at a current rate of 0.1C. The charge–discharge cycles were performed using constant current (CC) and constant voltage (CV) modes to evaluate critical performance metrics such as capacity retention, energy efficiency, and cycle life.

CHAPTER 4

RESULTS AND DISCUSSION

4.1 The Effect of the Die Exit Temperature on the Crystal Orientation of Precursor Film and Separator Morphology

During the precursor film preparation, die draw ratio (DDR) and die exit temperature play an important role in affecting crystallization structure. In terms of DDR, the extruded film is drawn by the chilled roll, which controls the DDR, then the lamellar structure shifts from spherulitic to more oriented row structure (Lei & Xu, 2017); Tabatabaei et al., 2009). From our preliminary observations, the oriented row structure was first observed at 140 DDR. Below this DDR, the oriented row structure cannot be detected. Due to the limitation of chilled roll speed, the maximum DDR was set at 180. In this study, the die exit temperature was observed between 215–245 °C.

Theoretically, a decrease in the die exit temperature results in faster cooling of the film. However, if the temperature is too low, it can negatively affect the film's surface quality, causing the solidified polymer to accumulate at the die exit, leading to uneven film thickness and rough surfaces. If the temperature drops too low, it may even cause blockages at the die exit. In this study, 215 °C is the lowest temperature at which film production was still possible. The effect of die exit temperature on the crystalline orientation factor *(Fc)* of precursor films was characterized by the polarized FTIR technique, as shown in Figure 4.1, the die exit temperature and DDR notably affect the Fc. The *Fc* values using the die exit temperature 215 °C are not involved by DDR. When the die exit temperature increases, the precursor film produced from 140 DDR presented a significant drop in *Fc*. For precursor films produced from 160 and 180 DDR, the die exit temperature has no considerable effect on Fc values. Moreover, it is clearly observed that the film produced from 160 DDR provided a higher Fc than 180 DDR in every die exit temperature. This reduction decreases because the excessive drawing speed damages the lamellae (Lei & Xu, 2017). This result suggests that 160 DDR is a suitable parameter in this study.

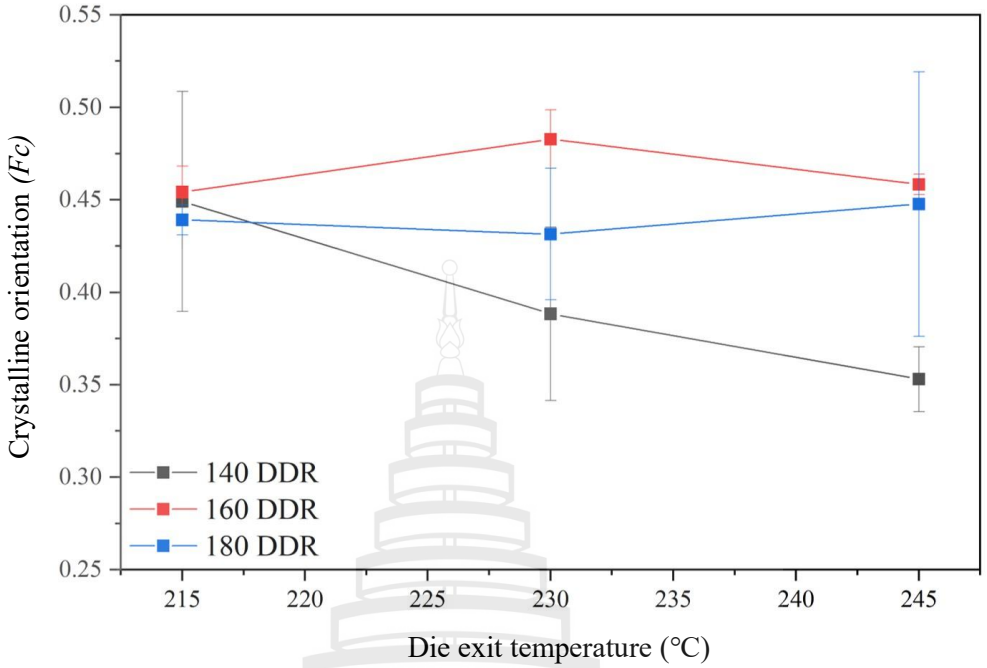

Figure 4.1 Comparison of *Fc* values from polarized FTIR of precursor films prepared at different die exit temperatures using a DDR range of 140-180.

Our findings align with those reported by Xu et al. (2018), who investigated how the die draw ratios (DDR) influences the crystalline orientation of polypropylene (PP) films, focusing on DDR values between 20 and 170. Their analysis utilized polarized FTIR and WAXD techniques. Results from polarized FTIR indicated that crystalline orientation improved with increasing DDR. However, at 170 DDR, crystalline orientation diminished as it reached a critical limit. This observation was corroborated by WAXD data, which showed a reduction in circularity at DDR 170.

This research observed the 2D-WAXS and our polarized FTIR results are consistent with the 2D-WAXS results shown in Figure 4.1 Generally, the 2D-WAXS pattern of spherulitic crystalline PP presents the ring formation on 110, 040, 130 and 111 planes (Xu et al., 2018). The increase in crystalline orientation transform the ring into an arc formation. The shorter the length of the arc, the higher the degree of crystalline orientation (Chandavasu et al., 2000). In comparison between die exit temperatures of 215°C to 245°C, the 2D-WAXS patterns obviously see the change of ring to arc formation. Figure 4.2 clearly shows that the diffraction rings remain nearly complete at a die exit temperature of 245°C, and the ring circularity decreases as the

temperature drops. Moreover, the 2D-WAXS result also confirmed that 160 DDR is a suitable parameter to produce precursor film due to short arc formation. Therefore, 160DDR was selected for further separator properties and battery performance tests.

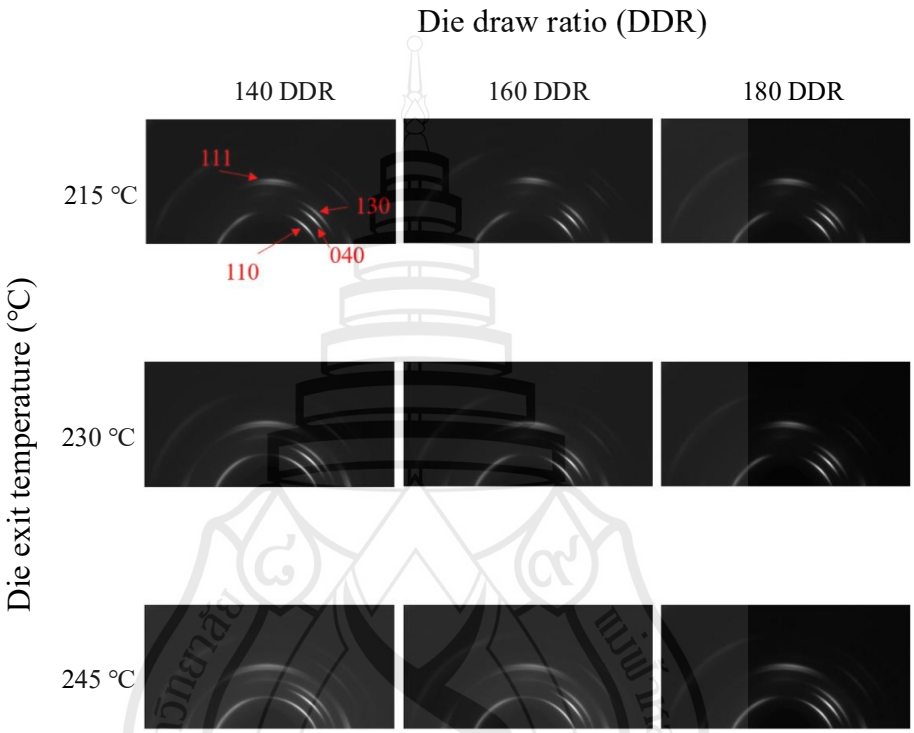

Figure 4.2 The 2D-WAXS patterns of precursor films prepared at different die exit temperatures using a DDR range of 140-180.

The die exit temperature was a key parameter on shear-induced crystalline of isotactic polypropylene (iPP). Farah and Bretas (2003) demonstrated the shear-induced crystallization of iPP in slit die using temperature range 169-230 °C and found that the shear-induced crystalline was particularly established near the die wall where the shear rate is the highest and the thickness of shear-induced crystalline layer increased at lower die temperature (Td) (Xu et al., 2015). At low die temperatures, such as 169°C, the cooling rate is high, allowing the polymer melt to crystallize more rapidly under shear. Additionally, at these low temperatures, the thickness of the crystalline layer increased along the length of the die due to the prolonged exposure to shear which facilitated continued crystallization. In contrast, at higher die

temperatures, such as 200°C or above, the crystallization process was significantly delayed due to reduced undercooling. The polymer remained in a molten state for a longer time, limiting the alignment and crystallization of the polymer chains. This led to thinner crystalline layers or, in some cases, the absence of shear-induced crystallization.

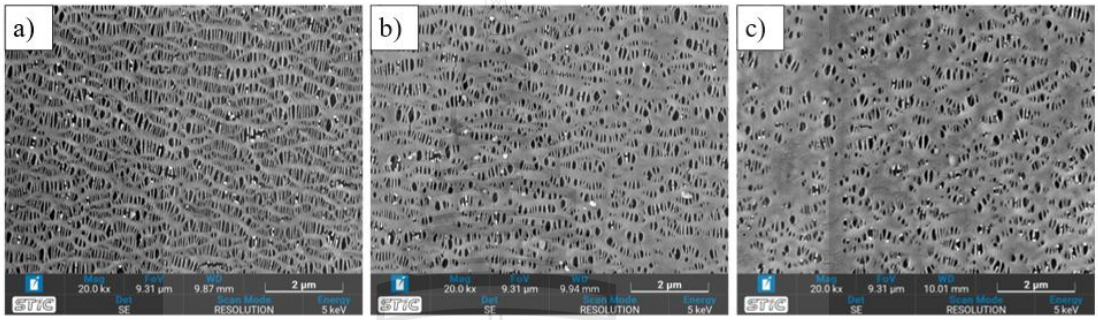

Figure 4.3 SEM images of membranes produced from precursor films (160 DDR) at different die exit temperatures: a) 215°C b) 230°C c) 245°C.

These findings underline that lower die temperatures favor the formation of shear-induced crystalline layers, while higher temperatures suppress this effect, emphasizing the importance of thermal conditions in extrusion processes. The effect of temperature on the formation of nuclei was also explored. Bednarek et al. (2021) found that low temperatures and shear enhance nucleation density and stabilize α- and β-phase nuclei in iPP. Lower temperatures favor β-phase formation (row-like lamellae) while higher temperatures favor α-phase formation (spherulite) as chain relaxation dominates, reducing β-phase stability (Mun & Won, 2021).

To investigate the effect of crystalline orientation on micropore formation in the separator at different die exit temperatures, the SEM technique was used and the image of the separator was produced from precursor films that were formed under different conditions are shown in Figure 4.3.

The SEM images in Figure 4.3 showed the porosity morphology of the separator produced from various die exit temperatures. It is evidenced to show that the separation of the lamellae structure during hot and cold stretching generated the pore morphology. For separator produced from die exit temperature 215°C, the pore size is

more oriented and uniform. But when the die exit temperature increases, twisted lamellae structures and non-uniform pores are observed and some areas present closed pores, which reduces porosity efficiency. It is noticed that high crystalline orientation precursor film offers good and uniform pore size. Xu et al. (2015) investigated the effect of melt-draw ratio (MDR) on the crystalline orientation and porosity of polypropylene membranes, focusing on the structural evolution and its impact on membrane performance and found a strong correlation between MDR, crystalline orientation, and porosity (Chandavasu et al., 2000). As the MDR increased, crystalline orientation improved significantly. This enhancement in orientation refined the lamellar structure and reduced defects, resulting in increased porosity. So, it is suggested that higher crystalline orientation leads to greater porosity. In this study, both the die exit temperature and DDR influence the crystalline orientation, which in turn affects the quality of the porosity. Reducing the die exit temperature promotes the formation of more nuclei, resulting in a higher crystalline orientation leading to better pore morphology.

4.2 The Effect of the Die Exit Temperature on Separator Morphology and Properties for Sinopec

The data in Table 4.1 illustrates the effect of die exit temperature on the pore size, shrinkage, and electrolyte uptake of separators. As the die exit temperature increases from 215°C to 245°C, the pore size and electrolyte uptake decrease, while the shrinkage percentages remain relatively low. At 215°C, the separator demonstrates the largest average pore size (0.265 ± 0.066 μm) and the highest electrolyte uptake (109.4 ± 4.4%). However, as the temperature rises to 230°C and 245°C, the average pore sizes shrink to 0.236 ± 0.070 μm and 0.197 ± 0.051 μm, respectively. Correspondingly, the electrolyte uptake drops significantly to 88.2 ± 16.6% and 41.0 ± 8.0%. The observed trend suggests that higher die exit temperatures lead to collapse pore structures, reducing the separator's ability to absorb electrolytes.

Table 4.1 Comparison of separator performance. The separators are produced from precursor films (160 DDR) at different die exit temperatures.

No.	Sample	Pore size (um)	Shrinkage (%)	Electrolyte Uptake (%)
1	215°C	0.265±0.066	5.8±3.5	109.4±4.4
2	230°C	0.236±0.070	2.0±2.9	88.2±16.6
3	245°C	0.197±0.051	2.8±2.7	41.0±8.0

Electrolyte uptake reflects the separator's ability to retain liquid electrolyte, which plays a critical role in supporting the electrochemical processes within the battery. The correlation between pore size and electrolyte uptake is evident, as smaller pore sizes at higher temperatures reduce the space for electrolyte retention. This finding aligns with Zhang et al. (2019) research, the study developed a nano-composite polymer electrolyte membrane (NCPE) by integrating a highly dispersed nano-TiO_2 hybrid with PVDF-HFP into glass fiber nonwoven, achieving a porosity of 58%, significantly higher than conventional PP separators 38%. This increased porosity enabled the NCPE to absorb 330% liquid electrolyte, compared to 55% for PP, highlighting a direct relationship between porosity and electrolyte uptake. Where separators with high porosity and interconnected pores demonstrate better electrolyte wettability and retention. Additionally, electrolyte uptake can serve as an indirect measure of separator porosity, quantifying the liquid absorbed into the pores a commonly used method in battery material research (Tabatabaei et al., 2009).

Table 4.2 Shows the values of charge and discharge testing for coin-type batteries. CR2032 half-cell uses a voltage range of 3.0 - 4.2 V and a charge density (C-rate) of 0.1C.

No.	Sample	Specific Capacity Charge (mAh/g)	Specific Capacity Discharge (mAh/g)	Chg/Dchg Efficiency (%)	Capacity (mAh)	Battery cycle
1	215°C	181.45	178.74	98.51	2.30	21
2	230°C	44.75	52.21	85.71	0.62	>50
3	245°C	84.751	97.73	86.72	1.16	32

Table 4.2 summarizes the charge and discharge characteristics of coin-type CR2032 half-cells using separators processed at varying die exit temperatures (215°C,

230°C, and 245°C). These separators were tested under a voltage range of 3.0 - 4.2 V with a charge density (C-rate) of 0.1C. Among the tested separators, the one processed at 215°C demonstrated superior performance with the highest specific capacities during charging (181.45 mAh/g) and discharging (178.74 mAh/g) and an impressive charge/discharge efficiency of 98.51%. The corresponding cell capacity was 2.30 mAh, with the cell maintaining stability for 21 cycles.

By comparison, commercial lithium-ion batteries typically achieve specific capacities ranging from 140 to 170 mAh/g for cathode materials such as $LiCoO_2$ and $LiNiMnCoO_2$ at similar C-rates (Manthiram, 2020). This suggests that the separator processed at 215°C performs competitively in terms of specific capacity, while its efficiency exceeds that of many commercial cells, which often exhibit charge/discharge efficiencies between 95% and 98% due to electrolyte degradation and electrode polarization.

The separator processed at 230°C, however, exhibited drastically reduced performance, with specific capacities of 44.75 mAh/g (charge) and 52.21 mAh/g (discharge), and a charge/discharge efficiency of only 85.71%. Despite this, it demonstrated better cycle life, sustaining over 50 cycles. Commercial lithium-ion batteries often achieve cycle lives exceeding 500–1000 cycles under similar conditions, highlighting the importance of further optimizing separator properties and ensuring compatibility with electrodes to extend cycle life without compromising capacity.

The separator processed at 245°C achieved moderate improvements over the 230°C sample, with specific capacities of 84.75 mAh/g (charge) and 97.73 mAh/g (discharge) and a charge/discharge efficiency of 86.72%. However, it remained below the performance of both the 215°C separator and commercial separators, which generally provide stable performance with minimal polarization over several hundred cycles.

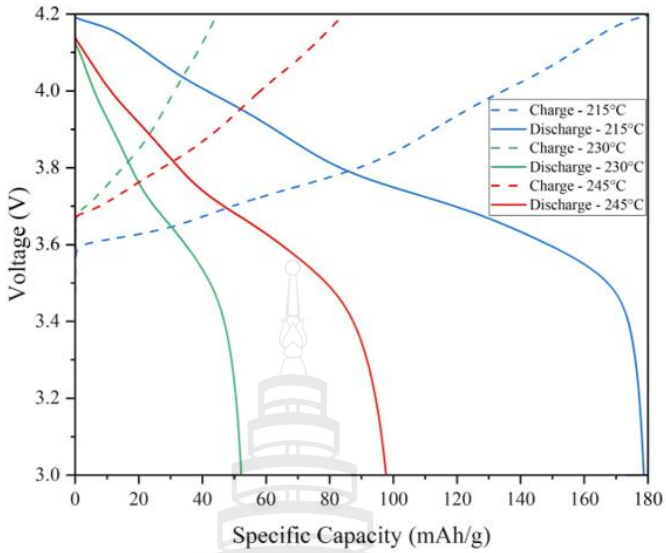

Figure 4.4 Galvanostatic Charge-Discharge profile of separators from coin-type batteries. CR2032 half-cell uses a voltage range of 3.0 – 4.2 V and a charge density (C-rate) of 0.1C.

Figure 4.4 shows the galvanostatic charge-discharge profiles for separators processed at different die exit temperatures. The separator processed at 215°C displayed the highest specific capacity (~180 mAh/g) and a stable voltage plateau, indicative of efficient lithium intercalation and deintercalation. Its excellent performance is attributed to superior electrolyte uptake (109.4 ± 4.4%) and a larger pore size (0.265 ± 0.066 μm), enhancing ionic conductivity and reducing polarization. These characteristics make it comparable to commercial polypropylene or polyethylene separators, which feature high porosity and uniform pore structures to maximize ionic transport.

In contrast, the separator processed at 230°C exhibited significant limitations, with reduced specific capacity (~50 mAh/g) and irregular voltage profiles. Lower electrolyte uptake (88.2 ± 16.6%) and smaller pore size (0.236 ± 0.070 μm) contributed to increased resistance and restricted lithium-ion mobility. Such limitations are less common in commercial separators, which are engineered for consistent porosity and superior electrolyte compatibility.

The separator processed at 245°C demonstrated intermediate performance, with specific capacity (~90 mAh/g) higher than the 230°C sample but much lower

than both the 215°C sample and commercial counterparts. Its smaller pore size (0.197 ± 0.051 μm) and significantly reduced electrolyte uptake (41.0 ± 8.0%) limited its ability to support efficient ionic transport, causing steep polarization and efficiency loss. Commercial separators generally avoid these issues by employing controlled thermal and mechanical processing to achieve optimized structural properties.

These results align with Kim et al. (2019), who emphasized that high porosity and superior electrolyte uptake are critical for enhanced ionic conductivity and stable cycling performance (Kim et al., 2019). Their findings showed that protonated TOCN membranes (TOCN-COOH) achieved 94.5% capacity retention after 100 cycles, outperforming their sodium carboxylated counterparts (TOCN-$COO^{-}Na^{+}$). The superior performance of these membranes highlights the importance of optimized separator properties for competitive battery performance.

In summary, the separator processed at 215°C demonstrated performance on par with commercial lithium-ion battery separators in terms of specific capacity and charge/discharge efficiency, though further improvements are required to match the extended cycle life and broader compatibility of commercial options. These findings underline the importance of precisely controlling thermal processing conditions during separator fabrication to achieve the structural and electrochemical properties necessary for high-performance lithium-ion batteries.

4.3 The Effect of the Die Exit Temperature on Separator Morphology and Properties from Domestic Raw Materials (IRPC S1003)

Previous parts (4.1 & 4.2) of this thesis, the effect of die exit temperature on polypropylene separators fabricated from Sinopec PPH-T03-S was systematically investigated. The results revealed that thermal processing parameters significantly influence crystalline orientation, pore morphology, and overall battery performance. Among the tested processing conditions, a die draw ratio (DDR) of 160 was identified as the most appropriate, producing well-oriented lamellae and uniform pores that supported enhanced electrolyte uptake and stable electrochemical behavior. These

findings established a solid foundation for understanding how die exit temperature governs the structural evolution and performance of polypropylene-based separators.

Building upon these insights, this part focuses on IRPC S1003, a polypropylene resin manufactured in Thailand. This grade was selected because it is a domestically produced homopolymer polypropylene with physical and molecular characteristics comparable to the imported Sinopec PPH-T03 resin, including similar density, melt flow rate (MFR), and crystallinity as shown in Table 4.3. The use of S1003 allows for evaluating the feasibility of substituting imported materials with local alternatives, thereby promoting cost efficiency and sustainability in the battery manufacturing industry. By adopting the optimized processing condition of DDR 160 identified in the previous investigation, this part examines the effect of die exit temperature on the morphological and electrochemical properties of separators prepared from IRPC S1003.

Table 4.3 Comparative properties of polypropylene resins for lithium-ion battery separator fabrication.

Property	Standard	Unit	Sinopec PPH-T03	1102H Lot. 0220604043	B1101 Lot. 02205025	1102K Lot. 0220604021	1100NK Lot. 0220504028	S1003 Lot. 02209055
Density	ISO 1183	g/cm^3	0.9054	0.9048	0.9034	0.9	0.902	0.9
MFR (2.16/230)	ISO 1133	g/10min	2.46	1.68	0.94	4.12	11	3.41
Flexural modulus, 23°C	ISO 178	MPa	1645	1840	1858	1650	1490	1658
Flexural strength	ISO 178	MPa	47	51	52	47	42	48
Charpy notched impact, 23°C	ISO 179/1A	kJ/m^2	4.98	6.66	7.82	3.75	3.18	3.48
Tensile strength @ Y	ISO 527	MPa	37.2	37.0	36.7	36.5	33.0	36.3
Tensile strength @ B	ISO 527	MPa	17.9	19	23.1	17	15	18.0
Elongation @ Y	ISO 527	%	8	8	8	8	7	8
Elongation @ B	ISO 527	%	70	65	75	80	68	93
HDT Flatwise. 0.45 Mpa	ISO 75-2	°C	96.8	108.4	106.5	98	94	94.9
Mw		g/mol	374500	485177	530356	352872	278785	365800
Mn		g/mol	52500	92743	103326	42051	42810	47900
Mw/Mn			7.14	5.23	5.13	8.39	6.51	7.63
Mz		g/mol	1417700	1554692	1371557	1301565	1074509	1011600
Mp		g/mol	325600	340340	401673	211941	161804	318100
Mv		g/mol	256700	423046	468405	302950	239119	250100
IVmwd		dL/g	2.7926	3.4540	3.7086	2.64	2.1951	2.7423
Tm		°C	166.1	167.96	168.91	166.32	165.73	167.59
Tc		°C	120.3	116.39	113.18	113.77	119.87	116.28
Crystallinity		%	49.4	46.59	45.87	46.54	46.34	52.87
Isotacticity index			98.1	98.6	98.7	98.5	98.3	98.5

This comparative approach provides both scientific and practical benefits. Scientifically, it extends the understanding of how die exit temperature affects polypropylene separators across different resin sources. Practically, it addresses the potential of using domestically produced PP to fabricate high-performance separators, thereby reducing reliance on imported materials and supporting local industrial development. Through the integration of structural analysis and battery performance evaluation, this part aims to clarify the feasibility of IRPC S1003 as a material for advanced lithium-ion battery separators.

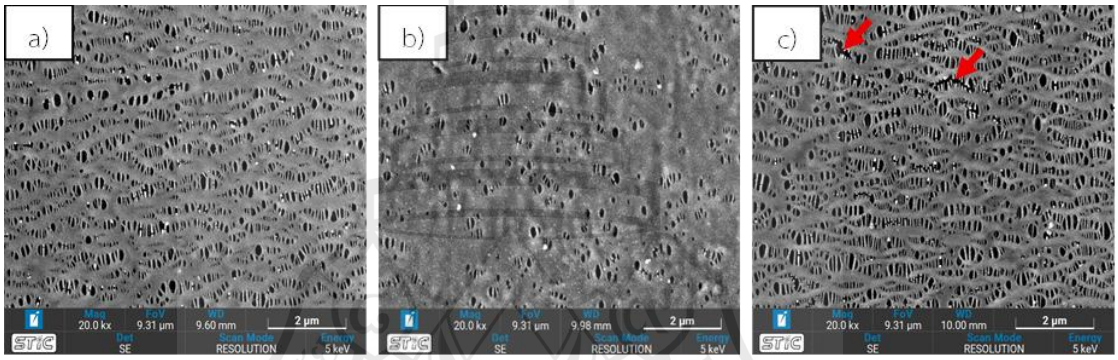

Figure 4.5 SEM images of IRPC S1003 membranes prepared under UTM conditions (DDR 160, C20% H100%) at different die exit temperatures: (a) 215 °C, (b) 230 °C, and (c) 245 °C. The red arrows indicated interconnected pores.

Table 4.4 Comparison separator performance of IRPC S1003. The separators are produced from precursor films (160 DDR) at different die exit temperatures.

No.	Sample (die exit temperature)	Pore size (um)	Shrinkage (%)	Electrolyte Uptake (%)
1	215°C	0.215 ± 0.050	3.3	71.3 ± 12.4
2	230°C	0.179 ± 0.049	1.5	69.2 ± 21.8
3	245°C	0.207 ± 0.064	5.8	104.2 ± 5.9

The effect of die exit temperature on the morphology and electrolyte uptake of IRPC S1003 membranes prepared under UTM conditions (cold stretching 20%, hot stretching 100%) is shown in Figure 4.5. At 215 °C of die exit temperature (Figure 4.5(a), the membrane exhibited elongated and slit-like pores with relatively uniform

distribution. The measured pore size was 0.215 ± 0.050 μm, shrinkage was 3.3%, and electrolyte uptake was 71.3 ± 12.4% (Table 4.4). This morphology reflects effective lamella separation and fibril formation, which provides continuous pathways for electrolyte penetration.

At 230 °C Figure 4.5(b), the pore structure became less uniform, with smaller and rounder pores. The pore size decreased to 0.179 ± 0.049 μm, and electrolyte uptake dropped to 69.2 ± 21.8%, while shrinkage was reduced to 1.5%. This suggests that partial chain relaxation during extrusion suppressed lamella disruption, limited pore propagation, and reduced porosity, ultimately restricting electrolyte absorption (Castejón et al., 2018).

At the highest die exit temperature of 245 °C Figure 4.5(c), the membrane showed elongated and interconnected pores as presented in red arrows, more open than those at 230 °C. The pore size increased to 0.207 ± 0.064 μm, and electrolyte uptake rose significantly to 104.2 ± 5.9%, while shrinkage also increased to 5.8%. These results suggest that higher thermal energy facilitated lamella reorganization (Li et al., 2018) and pore expansion, thereby enhancing electrolyte wettability but at the cost of reduced dimensional stability.

Table 4.5 Shows the values of charge and discharge testing for IRPC S1003 coin-type batteries. CR2032 half-cell uses a voltage range of 3.0 - 4.2 V and a charge density (C-rate) of 0.1C.

No.	Sample	Specific Capacity Charge (mAh/g)	Specific Capacity Discharge (mAh/g)	Chg/Dchg Efficiency (%)	Capacity (mAh)	Battery cycle
1	215°C	180.26	176.41	97.86	2.295	13
2	230°C	1.00	1.67	59.88	0.013	>50
3	245°C	The measures could not be obtained due to internal short-circuiting				

The battery performance of coin-type cells assembled with IRPC S1003 separators fabricated at different die exit temperatures is summarized in Table 4.5. At 215 °C, the separator demonstrated promising battery performance, achieving a charge capacity of 180.26 mAh/g and a discharge capacity of 176.41 mAh/g, corresponding to a high charge–discharge efficiency of 97.86%. The total cell capacity reached 2.295 mAh, with the battery sustaining 13 charge–discharge cycles before significant

degradation. These results suggest that the separator prepared at lower die exit temperature maintained sufficient pore connectivity and electrolyte uptake to support efficient lithium-ion transport, thereby providing stable capacity and high efficiency.

In contrast, the separator fabricated at 230 °C showed a drastic decline in performance. The charge and discharge capacities decreased to 1.00 mAh/g and 1.67 mAh/g, respectively, with an efficiency of only 59.88%. The overall cell capacity was reduced to 0.013 mAh, despite the fact that the battery could technically sustain more than 50 cycles. This phenomenon can be explained by the severely reduced pore size and low electrolyte uptake observed at this temperature (0.179 ± 0.049 μm and 69.2 ± 21.8%, respectively (Table 4.5). The limited ionic pathways restricted charge storage and transport, leading to very low specific capacities. However, the reduced dimensional change (shrinkage 1.5%) provided mechanical stability, which likely explains the extended cycle count despite poor electrochemical efficiency.

Furthermore, the cycling behavior also reflected the trade-off between ionic conductivity and structural integrity. Although the 215 °C separator exhibited excellent capacity and efficiency, its cycle life was limited to 13 cycles due to dimensional instability and gradual pore deformation during repeated lithiation and delithiation. In contrast, the 230 °C separator, despite its very low capacity, maintained over 50 cycles, suggesting that improved dimensional stability effectively prevented mechanical degradation or short-circuiting. This indicates that excessive porosity can accelerate structural fatigue, while too compact a morphology suppresses electrochemical activity but prolongs cell lifespan. Similar relationships between separator microstructure and cycling durability have been reported in previous studies. Li et al. (2018) demonstrated that polypropylene/polyethylene multilayer separators with optimized porosity and electrolyte uptake exhibited enhanced capacity retention over extended cycling. Liu et al. (2021) further emphasized that mechanical and thermal stability of separators plays a decisive role in preventing internal short circuits, thereby improving cycle life. In addition, Kannan et al. (2018) reported that separator thickness and pore connectivity directly influence ionic conductivity and long-term cell stability. These findings are consistent with the present results, confirming that the balance between ionic transport and dimensional stability is crucial for achieving both high capacity and prolonged cycling performance.

At the highest die exit temperature of 245 °C, no functional coin cells could be assembled, as the separator led to internal short circuits during testing. This failure can be attributed to the unstable pore structure observed at this condition. Although the measured electrolyte uptake was high (104.2 ± 5.9%), the increased shrinkage (5.8%) and irregular pore connectivity likely compromised the separator's integrity, allowing electrode contact and causing short-circuiting during cell operation.

These findings emphasize the critical role of die exit temperature in determining the electrochemical performance of polypropylene separators. Lower temperature (215 °C) supports balanced morphology and ionic conductivity, leading to high specific capacity and efficiency, while intermediate temperature (230 °C) restricts ion transport due to suppressed pore formation, resulting in severe capacity loss despite stable cycling. Excessively high temperature (245 °C) compromises separator stability, preventing its application in functional cells. This trend is consistent with prior studies, where separator porosity and electrolyte wettability have been directly correlated with improved capacity retention and cycling stability (Kim et al., 2019; S. Zhang et al., 2015) showing that good porosity and electrolyte wettability are vital for stable cycling. In short, careful control of the processing temperature is the key to making reliable, high-performance separators from local polypropylene like IRPC S1003.

When compared with the membrane fabricated from Sinopec PPH-T03-S at die exit temperature 215 °C, clear differences were observed in both morphology and performance. The Sinopec separator exhibited larger pores (0.265 ± 0.066 μm) and higher electrolyte uptake (109.4 ± 4.4%) than IRPC S1003 (0.215 ± 0.050 μm, 71.3 ± 12.4%). In addition, the Sinopec membrane delivered a slightly higher discharge capacity (178.74 mAh/g vs. 176.41 mAh/g) and longer cycle life (21 vs. 13 cycles), indicating more stable ionic transport and mechanical integrity.

The performance differences between the two polypropylene resins can be clearly explained by their distinct molecular characteristics. Sinopec PPH-T03-S exhibits a lower melt flow rate (2.46 g/10 min) and higher molecular weight (Mw = 374,500 g/mol), together with a larger fraction of ultra-long chains (Mz = 1,417,700 g/mol). These features promote strong chain entanglement and maintain a stable lamellar orientation during stretching, forming elongated and interconnected pores

(Sadeghi et al., 2007b; Xu et al., 2018). As a result, the Sinopec-based separators show higher electrolyte uptake and better cycling stability.

In contrast, IRPC S1003 possesses higher crystallinity (52.87% vs. 49.4%), which increases lamellar stiffness and restricts controlled deformation during stretching (Lei et al., 2018). Moreover, its lower number-average molecular weight (Mn = 47,900 g/mol) and broader molecular weight distribution (Mw/Mn = 7.63) indicate a larger fraction of short chains. These short chains weaken entanglement uniformity and promote premature lamella fracture, producing smaller and less-connected pores that hinder ion transport (Lei et al., 2018; Xu et al., 2018). Consequently, the IRPC S1003 separators exhibit reduced electrolyte wettability and lower electrochemical capacity compared with those made from Sinopec PPH-T03-S.

These findings are consistent with earlier studies that investigated how molecular parameters influence lamellar development and pore formation. Sadeghi et al. (2007) compared polypropylene grades with different molecular weights and molecular weight distributions, reporting that moderate Mw (~416 kg/mol) and broad Mw/Mn (~5.2) produced well-connected pores due to a balance between lamella integrity and chain mobility. Xu et al. (2018) examined films with varying Mw under different draw ratios and found that high Mw enhanced lamellar orientation and mechanical strength, but excessive rigidity suppressed pore growth. Similarly, Lei et al. (2018) compared PP samples with different crystallinity levels and concluded that balanced crystallinity (~50%) and adequate chain mobility were essential for lamella-to-fibril transformation, whereas excessive rigidity hindered pore expansion.

In summary, the differences between Sinopec PPH-T03-S and IRPC S1003 can be directly explained by their molecular characteristics. Sinopec's favorable molecular weight and chain entanglement promote the formation of open, interconnected pores that support high electrolyte uptake and long cycle life. IRPC, while locally produced and advantageous for supply-chain independence, has intrinsic molecular features, higher crystallinity, lower Mn, and broader Mw/Mn that restrict pore propagation and limit electrochemical stability. These results show that the basic properties of the resin—such as MFR, molecular weight (Mw and Mn), molecular weight distribution (Mw/Mn), and crystallinity play a key role in shaping the structure and overall

performance of polypropylene separators used in lithium-ion batteries (Lei et al., 2018; Sadeghi et al., 2007b; Xu et al., 2018).

4.4 Scale-up of Polypropylene Battery Separator Production via Dry Stretching

In Part 4.1- 4.3 of this thesis, the effects of die exit temperature on polypropylene separators fabricated from Sinopec PPH-T03-S and IRPC S1003 were systematically investigated using laboratory-scale uniaxial tensile machine (UTM) processing. These studies demonstrated that thermal processing conditions strongly influenced pore morphology, electrolyte uptake, and electrochemical performance, with the optimal processing condition identified at a die draw ratio (DDR) of 160 and die exit temperature of 215 °C. Comparisons between Sinopec and IRPC revealed that while Sinopec exhibited superior pore structure and higher electrolyte uptake, IRPC showed competitive performance under optimized conditions, indicating its potential as a locally produced alternative for lithium-ion battery separator applications.

Building upon these findings, Part 4.4 extends the research from laboratory-scale trials to pilot-scale production using a machine direction orientation (MDO) system. The MDO process, commonly employed in industrial film manufacturing, provides a continuous and scalable stretching method that more closely represents commercial production conditions compared to UTM. By directly comparing membranes produced from Sinopec and IRPC resins under MDO processing, this part aims to evaluate not only the scalability of the dry-stretching technique but also the industrial feasibility of using IRPC S1003 as a separator material.

This investigation will focus on examining the morphological characteristics, electrolyte uptake, and electrochemical performance of MDO-fabricated membranes, and comparing them with those obtained from UTM in earlier parts of this thesis. Through this approach, Part 4.4 provides critical insights into the transition from laboratory optimization to pilot-scale validation, ensuring that the results are relevant to practical manufacturing and commercial applications.

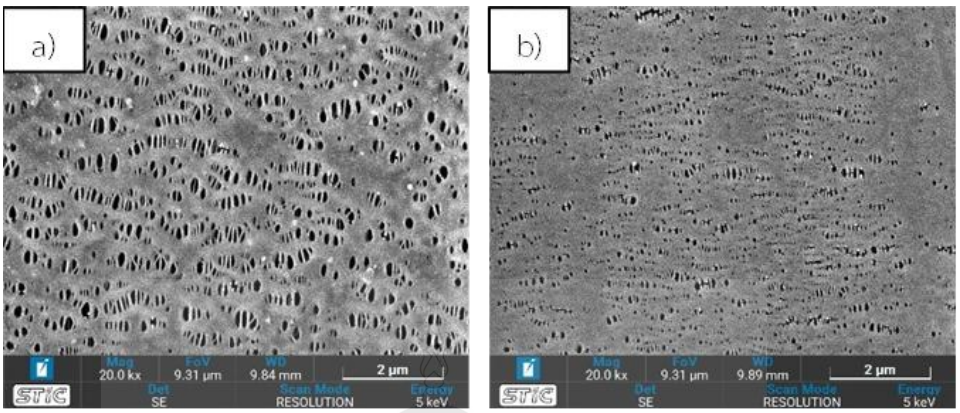

Figure 4.6 The SEM images of membranes produced by MDO a) Sinopec PPH-T03-S and b) IRPC S1003.

Table 4.6 MDO comparison separator performance. The separators are produced from precursor films (160 DDR) at different die exit temperatures.

No.	Sample	Pore size (um)	Shrinkage (%)	Electrolyte Uptake (%)
1	Sinopec PPH-T03-S 215°C	0.124 ± 0.050	5.7	89.8 ± 4.4
2	IRPC S1003 215°C	0.127 ± 0.043	4.6	84.3 ± 10.4

The scale-up of separator production using a Machine Direction Orientation (MDO) system was evaluated and compared to laboratory-scale Uniaxial Tensile Machine (UTM) processing. Representative SEM images of Sinopec PPH-T03-S and IRPC S1003 membranes fabricated by MDO are shown in Figure 4.6 with corresponding structural data summarized in Table 4.6.

For Sinopec PPH-T03-S, the MDO-processed membrane (Figure 4.6(a)) displayed relatively fine and uniformly distributed pores with an average size of 0.124 ± 0.050 µm, shrinkage of 5.7%, and electrolyte uptake of 89.8 ± 4.4%. Compared with the UTM membrane at 215 °C (Figure 4.3(a)), Part 4.1*)*, which exhibited larger pores (0.265 ± 0.066 µm) and higher electrolyte uptake (109.4 ± 4.4%), the MDO sample showed reduced pore size and slightly lower uptake. This difference likely originates from the continuous stretching mechanism in the MDO process, which imposes uniform tension along the machine direction and limits excessive fibril relaxation during deformation (Zhang, 2007).

Similarly, for IRPC S1003, the MDO membrane (Figure 4.6(b)) exhibited pores averaging 0.127 ± 0.043 μm with shrinkage of 4.6% and electrolyte uptake of 84.3 ± 10.4%. By comparison, the UTM sample at 215 °C (Figure 4.5(a)) showed larger pores (0.215 ± 0.050 μm) and higher uptake (71.3 ± 12.4%). Interestingly, while pore size decreased significantly in the MDO membrane, the electrolyte uptake did not decline as drastically and even remained comparable, suggesting that the improved pore alignment in the MDO process compensated for the smaller pore size by maintaining effective ionic pathways (Zhang, 2007).

These results demonstrate that MDO processing produced membranes with slightly smaller and denser pores compared to those prepared by UTM. Despite the reduction in pore size, both Sinopec and IRPC membranes maintained satisfactory electrolyte absorption, while showing notably lower shrinkage. The improvement in dimensional stability is attributed to the continuous and uniform tension applied during MDO stretching, which restricts excessive pore growth and fibril relaxation. For IRPC S1003, the MDO process even enhanced electrolyte uptake relative to its UTM counterpart, likely due to improved pore alignment and interconnectivity that facilitated electrolyte penetration. Overall, these findings indicate that the MDO process effectively balances structural stability and electrolyte wettability, making it more suitable for scalable separator fabrication. Both Sinopec and IRPC resins demonstrated good compatibility with MDO-based scale-up, with Sinopec still offering higher electrolyte uptake, while IRPC S1003 achieved competitive and stable performance as a promising local resin for lithium-ion battery separator manufacturing.

The electrochemical performance of separators prepared from Sinopec PPH-T03-S and IRPC S1003 resins using the MDO process is summarized in Table 4.7. For comparison, reference data from UTM-processed membranes are also included from Part 4.1 (Table 4.2, No. 1) and Part 4.3 (Table 4.5, No. 1). This comparison highlights the influence of scale-up processing and resin type on the charge–discharge behavior of CR2032 half-cells.

Table 4.7 Shows the values of charge and discharge testing for coin-type batteries. CR2032 half-cell uses a voltage range of 3.0 - 4.2 V and a charge density (C-rate) of 0.1C. MDO.

No.	Sample	Specific Capacity Charge (mAh/g)	Specific Capacity Discharge (mAh/g)	Chg/Dchg Efficiency (%)	Capacity (mAh)	Battery cycle
1	Sinopec PPH-T03-S 215°C	172.38	172.17	99.88	2.289	>50
2	IRPC S1003 215°C	169.06	167.9	99.31	2.361	>50

For Sinopec PPH-T03-S, the UTM-prepared separator at 215 °C (Part 4.2, Table 4.2 No. 1) delivered a charge capacity of 181.45 mAh/g and a discharge capacity of 178.74 mAh/g with an efficiency of 98.51%, corresponding to a cell capacity of 2.30 mAh and a cycle life of 21 cycles. When processed by MDO under equivalent conditions (Table 4.7), the specific capacities decreased slightly to 172.38 mAh/g (charge) and 172.17 mAh/g (discharge). However, the charge/discharge efficiency improved significantly to 99.88%, and the cycle life was extended to more than 50 cycles. This indicates that although MDO membranes exhibited smaller pores and slightly reduced uptake compared to UTM (Table 4.7 vs. Part 4.2, Table 4.3), the improved morphological stability under MDO provided long-term cycling durability and higher coulombic efficiency. This improvement can be attributed to the formation of uniformly oriented lamellae and interconnected fibrillar structures during continuous MDO stretching, which enhance mechanical integrity and suppress pore collapse or separator shrinkage during repeated charge–discharge cycles (Zhang, 2007).

A similar trend was observed for IRPC S1003. The UTM separator at 215 °C (Part 4.3, Table 4.5 No. 1) achieved charge and discharge capacities of 180.26 mAh/g and 176.41 mAh/g, respectively, with an efficiency of 97.86%, a total cell capacity of 2.295 mAh, and 13 stable cycles. By contrast, the MDO separator (Table 4.7) demonstrated slightly lower specific capacities of 169.06 mAh/g (charge) and 167.9 mAh/g (discharge), but the charge/discharge efficiency improved to 99.31%, with the

cycle life extending beyond 50 cycles. This improvement highlights the stabilizing effect of MDO processing, which reduces pore collapse and dimensional shrinkage, thereby prolonging separator integrity during cycling.

Comparing the two resins under MDO conditions, Sinopec showed marginally higher specific capacities (172.17 mAh/g vs. 167.9 mAh/g) and slightly better efficiency (99.88% vs. 99.31%), while IRPC achieved a higher absolute cell capacity (2.361 mAh vs. 2.289 mAh). Both resins demonstrated robust long-term cycling with more than 50 cycles, in contrast to their UTM-processed counterparts where cycle life was limited (21 cycles for Sinopec and 13 cycles for IRPC.

These results show that although the UTM process produced slightly higher initial capacities because of its larger pores and higher electrolyte uptake, the MDO process provided better long-term stability and higher efficiency thanks to its more uniform and well-controlled stretching. In addition, the results indicate that even though IRPC S1003 has some molecular limitations compared with Sinopec, it can still be processed effectively by MDO to deliver similar electrochemical performance and stable cycling. This suggests that IRPC S1003 has good potential as a practical local material for lithium-ion battery separator production.

CHAPTER 5

CONCLUSION

This study explored how the die exit temperature affects the structure and performance of polypropylene (PP) battery separators made from both imported (Sinopec PPH-T03-S) and local (IRPC S1003) resins, and also examined how the process can be scaled up using an MDO system.

From the lab-scale tests, the best condition was found at a die draw ratio (DDR) of 160 and a die exit temperature of 215 °C. Under this setting, the Sinopec separator had well-aligned lamellae, uniform pores, high electrolyte uptake, and excellent battery performance, showing a discharge capacity around 179 mAh/g with high efficiency (about 98.5%). When the temperature increased to 230–245 °C, the pores became less connected, electrolyte absorption dropped, and the battery performance declined.

For the local IRPC S1003 resin, the same trend was seen. The separator made at 215 °C showed good pore structure and stable ionic flow, giving similar performance to Sinopec. But when the temperature rose to 230 °C, its performance fell sharply, and at 245 °C the separator failed due to internal short-circuits. Compared with Sinopec, the IRPC separator had smaller pores and lower electrolyte uptake, mainly because of its higher crystallinity and wider molecular weight distribution. Even so, when processed properly, the IRPC material still performed well and showed promise as a local alternative.

When the process was scaled up using the MDO system, both materials produced membranes with finer and more uniform pores, better dimensional stability, and longer cycle life. Although the capacity was slightly lower than the lab-made samples, the efficiency reached nearly 99%, and the batteries ran stably for more than 50 cycles. This shows that MDO processing gives stronger, more durable separators suitable for large-scale production.

In summary, careful control of the die exit temperature and stretching method is key to getting the right balance between porosity, electrolyte uptake, and mechanical

strength. The MDO process worked well for scale-up, and the local IRPC S1003 resin proved capable of delivering performance close to imported materials making it a good option for practical, locally sourced lithium-ion battery separator production.

REFERENCES

Abraham, K. M. (1993). Directions in secondary lithium battery research and development. *Electrochimica Acta, 38*(9), 1233–1248. https://doi.org/10.1016/0013-4686(93)85083-B

Arora, P., & Zhang, Z. (2004). Battery separators. *Chemical Reviews*, *104*(10), 4419-4462. https://doi.org/10.1021/cr020738u

Cai, Q., Xu, R., Chen, X., Chen, C., Mo, H., & Lei, C. (2016). Structure and properties of melt-stretching polypropylene/silicon dioxide compound microporous membrane. *Polymer Composites*, *37*(9), 2684–2691. https://doi.org/10.1002/pc.23462

Castejón, P., Habibi, K., Saffar, A., Ajji, A., Martínez, A. B., & Arencón, D. (2018). Polypropylene-based porous membranes: Influence of polymer composition, extrusion draw ratio and uniaxial strain. *Polymers, 10*(1), 33. https://doi.org/10.3390/polym10010033

Chandavasu, C., Xanthos, M., Sirkar, K. K., & Gogos, C. G. (2000). Preparation of microporous films from immiscible blends via melt processing. *Journal of Plastic Film and Sheeting*, *16*(4), 288–299. https://doi.org/10.1106/VEHN-PMN3-Q6RE-FUH9

Cui, J., Liu, J., He, C., Li, J., & Wu, X. (2017). Composite of polyvinylidene fluoride–cellulose acetate with Al(OH)3 as a separator for high-performance lithium ion battery. *Journal of Membrane Science*, *541*, 661–667. https://doi.org/10.1016/j.memsci.2017.07.048

Deimede, V., & Elmasides, C. (2015). Separators for lithium-ion batteries: A review on the production processes and recent developments. *Energy Technology*, *3*(5), 453–468. https://doi.org/10.1002/ente.201402215

Ding, L., Xu, R., Pu, L., Yang, F., Wu, T., & Xiang, M. (2019). Pore formation and evolution mechanism during biaxial stretching of β-iPP used for lithium-ion batteries separator. *Materials & Design, 179,* 107880. https://doi.org/10.1016/j.matdes.2019.107880

Goodenough, J. B., & Park, K. S. (2013). The Li-ion rechargeable battery: A perspective. *Journal of the American Chemical Society, 135*(4), 1167–1176. https://doi.org/10.1021/ja3091438

Huang, X. (2011). Separator technologies for lithium-ion batteries. *Journal of Solid State Electrochemistry, 15*(4), 649–662. https://doi.org/10.1007/s10008-010-1264-9

Ikezaki, K., Kaneko, T., & Sakakibara, T. (1981). *Effect of crystallinity on electrical conduction in polypropylene*. *Japanese Journal of Applied Physics, 20*(3), 609–615. https://doi.org/10.1143/JJAP.20.609

Johnson, M. B., & Wilkes, G. L. (2002). Microporous membranes of isotactic poly(4-methyl-1-pentene) from a melt-extrusion process. II. Effects of thermal annealing and stretching on porosity. *Journal of Applied Polymer Science*, *84*(5), 1076–1100. https://doi.org/10.1002/app.10395

Kim, H., Guccini, V., Lu, H., Salazar-Alvarez, G., Lindbergh, G., & Cornell, A. (2019). Lithium ion battery separators based on carboxylated cellulose nanofibers from wood. *ACS Applied Energy Materials*, *2*(2), 1241–1250. https://doi.org/10.1021/acsaem.8b01797

Lee, H., Yanilmaz, M., Toprakci, O., Fu, K., & Zhang, X. (2014). A review of recent developments in membrane separators for rechargeable lithium-ion batteries. *Energy & Environmental Science, 7*(12), 3857–3886. https://doi.org/10.1039/C4EE01432D

Lei, C., & Xu, R. (2017). Melt-stretching polyolefin microporous membrane. In P. Bettotti (Ed.), *Submicron porous materials* (pp. 81–105). Springer International Publishing. https://doi.org/10.1007/978-3-319-53035-2_4

Lei, C., Wu, S., Xu, R., Cai, Q., Hu, B., Peng, X., & Shi, W. (2013). Formation of stable crystalline connecting bridges during the fabrication of polypropylene microporous membrane. *Polymer Bulletin*, *70*(4), 1353–1366. https://doi.org/10.1007/s00289-013-0933-0

Lei, C., Xu, R., Tian, Z., Huang, H., Xie, J., & Zhu, X. (2018). Stretching-induced uniform micropores formation: An in situ SAXS/WAXS study. *Macromolecules*, *51*(9), 3433–3442. https://doi.org/10.1021/acs.macromol.7b02335

Li, Y., Pu, H., & Wei, Y. (2018). Polypropylene/polyethylene multilayer separators with enhanced thermal stability for lithium-ion battery via multilayer coextrusion. *Electrochimica Acta*, *264*, 140–149. https://doi.org/10.1016/j.electacta.2018.01.114

Liu, K., Liu, Y., Lin, D., Pei, A., & Cui, Y. (2018). Materials for lithium-ion battery safety. Science Advances, 4(6), eaas9820. https://doi.org/10.1126/sciadv.aas9820

Liu, Z.-Y., Wu, X.-T., Yan, J., Yang, W., & Yang, M.-B. (2019). Effect of annealing temperature on PP microporous membranes obtained by a melt-extrusion-stretching method. *International Polymer Processing, 34*(4), 467–474. https://doi.org/10.3139/217.3774

Manthiram, A. (2020). A reflection on lithium-ion battery cathode chemistry. *Nature Communications, 11,* 1550. https://doi.org/10.1038/s41467-020-15355-0

Mun, S. C., & Won, J. H. (2021). Manufacturing processes of microporous polyolefin separators for lithium-ion batteries and correlations between mechanical and physical properties. *Crystals, 11*(9), 1013. https://doi.org/10.3390/cryst11091013

Palacín, M. R. (2009). Recent advances in rechargeable battery materials: A chemist's perspective. *Chemical Society Reviews*, *38*(9), 2565–2575. https://doi.org/10.1039/b820555h

Ren, Y., Zou, H., Wang, S., Liu, J., Gao, D., Wu, C., & Zhang, S. (2018). Effect of annealing on microstructure and tensile properties of polypropylene cast film. *Colloid and Polymer Science*, *296*(1), 41–51. https://doi.org/10.1007/s00396-017-4220-8

Xu, R., Xie, J., Tian, Z., Huang, H., Chen, X., Lei, C., & Zhu, X. (2018). Pore growth and stabilization in uniaxial stretching polypropylene microporous membrane processed by heat-setting. *Journal of Polymer Science, Part B: Polymer Physics*, *56*(24), 1604–1614. https://doi.org/10.1002/polb.24748

Sadeghi, F., Ajji, A., & Carreau, P. J. (2007a). Analysis of microporous membranes obtained from polypropylene films by stretching. *Journal of Membrane Science*, *292*(1–2), 62–71. https://doi.org/10.1016/j.memsci.2007.01.023

Sadeghi, F., Ajji, A., & Carreau, P. J. (2007b). Analysis of row nucleated lamellar morphology of polypropylene obtained from the cast film process: Effect of melt

rheology and process conditions. *Polymer Engineering and Science*, *47*(7), 1170–1178. https://doi.org/10.1002/pen.20837

Saffar, A., Carreau, P. J., Ajji, A., & Kamal, M. R. (2014). Influence of stretching on the performance of polypropylene-based microporous membranes. *Industrial and Engineering Chemistry Research*, *53*(36), 14014–14021. https://doi.org/10.1021/ie502300j

Scrosati, B., & Garche, J. (2010). Lithium batteries: Status, prospects and future. *Journal of Power Sources, 195*(9), 2419–2430. https://doi.org/10.1016/j.jpowsour.2009.11.048

Tabatabaei, S. H., Carreau, P. J., & Ajji, A. (2009). Effect of processing on the crystalline orientation, morphology, and mechanical properties of polypropylene cast films and microporous membrane formation. Polymer, 50(17), 4228–4240. https://doi.org/10.1016/j.polymer.2009.06.071

Tabatabaei, S. H., Carreau, P. J., & Ajji, A. (2009b). Microporous membranes obtained from PP/HDPE multilayer films by stretching. *Journal of Membrane Science*, *345*(1–2), 148–159. https://doi.org/10.1016/j.memsci.2009.08.038

Tarascon, J.-M., & Armand, M. (2001). Issues and challenges facing rechargeable lithium batteries. Nature, 414(6861), 359–367. https://doi.org/10.1038/35104644

Wang, S., Saffar, A., Ajji, A., Wu, H., & Guo, S.-Y. (2015). Fabrication of microporous membranes from melt extruded polypropylene precursor films via stretching: Effect of annealing. *Chinese Journal of Polymer Science (English Edition)*, *33*(7), 1028–1037. https://doi.org/10.1007/s10118-015-1643-x

Xu, K. (2014). Electrolytes and interphases in Li-ion batteries and beyond. *Chemical Reviews, 114*(23), 11503–11618. https://doi.org/10.1021/cr500003w

Xu, R., Chen, X., Xie, J., Cai, Q., & Lei, C. (2015). Influence of melt-draw ratio on the crystalline structure and properties of polypropylene cast film and stretched microporous membrane. *Industrial and Engineering Chemistry Research*, *54*(11), 2991–2999. https://doi.org/10.1021/acs.iecr.5b00215

Xu, R., Lei, C., Cai, Q., Hu, B., Shi, W., Mo, H., & Chen, C. (2014). Micropore formation process during stretching of polypropylene casting precursor film. *Plastics, Rubber and Composites*, *43*(8), 257–263. https://doi.org/10.1179/1743289814Y.0000000100

Xu, R., Zeng, S., Wang, J., Kang, J., Xiang, M., & Yang, F. (2018). Impact of different die draw ratio on crystalline and oriented properties of polypropylene cast films and annealed films. *Journal of Polymer Research, 25*(6), 142. https://doi.org/10.1007/s10965-018-1534-2

Yang, M., & Hou, J. (2012). Membranes in lithium ion batteries. *Membranes, 2*(3), 367–383. https://doi.org/10.3390/membranes2030367

Zhang, S., Cao, J., Shang, Y., Wang, L., He, X., Li, J., Zhao, P., & Wang, Y. (2015). Nanocomposite polymer membrane derived from nano TiO_2-PMMA and glass fiber nonwoven: High thermal endurance and cycle stability in lithium ion battery applications. *Journal of Materials Chemistry A*, *3*(34), 17697–17703. https://doi.org/10.1039/c5ta02781k

Zhang, S. S. (2007). A review on the separators of liquid electrolyte Li-ion batteries. *Journal of Power Sources*, *164*(1), 351–364. https://doi.org/10.1016/j.jpowsour.2006.10.065

APPENDIX

SUPPLEMENTARY INFORMATION

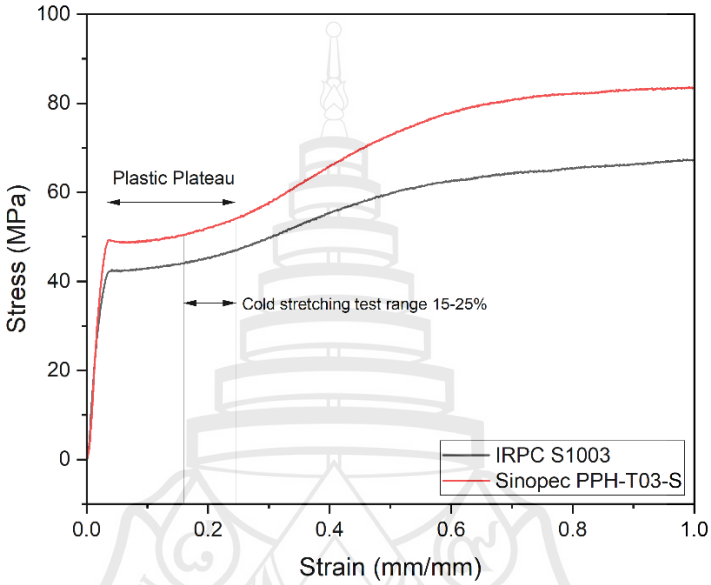

Figure A1 Stress – Strain curve of Sinopec PPH-T03-S (red) and IRPC S1003 (black)

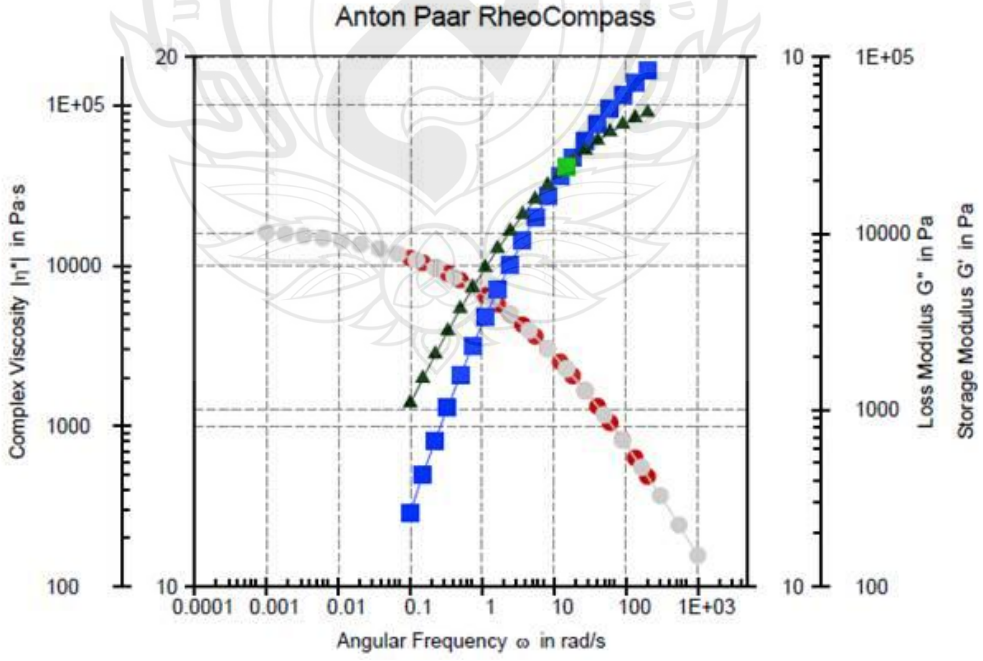

Figure A2 Complex viscosity graph of Sinopec PPH-T03-S

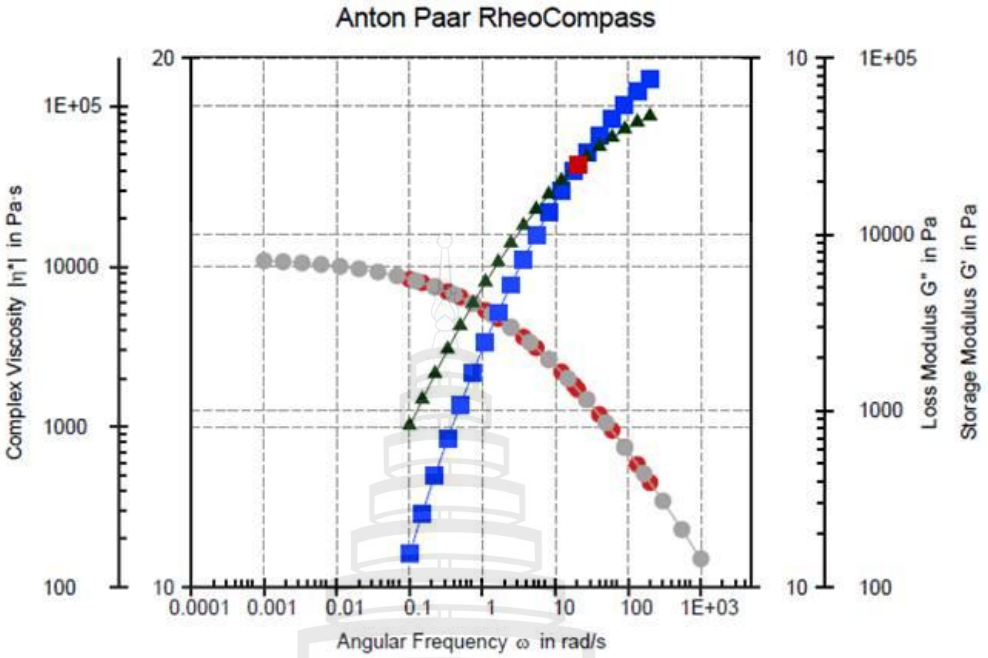

Figure A3 Complex viscosity graph of IRPC S1003